nature communications

Article

https://doi.org/10.1038/s41467-025-59476-w

PfPPM2 signalling regulates asexual division and sexual conversion of human malaria parasite *Plasmodium falciparum*

Received: 16 September 2024

Accepted: 24 April 2025

Published online: 23 May 2025

Check for updates

Akanksha Rawat[1], Neelam Antil[2], Meenakshi[1], Bhagyashree Deshmukh[3], Akhila Balakrishna Rai[2], Annu Nagar[1], Narendra Kumar[1,3], T. S. Keshava Prasad[2], Krishanpal Karmodiya[4] & Pushkar Sharma[1]

Malaria parasite undergoes interesting developmental transition in human and mosquito host. While it divides asynchronously in the erythrocytes, it switches to sexual forms, which is critical for disease transmission. We report a novel signalling pathway involving Protein Phosphatase PfPPM2, which regulates asexual division of *Plasmodium falciparum* as well as its conversion to sexual forms. PfPPM2 may regulate the phosphorylation of key proteins involved in chromatin remodelling and protein translation. One of the key PfPPM2-targets was Heterochromatin Protein 1 (HP1), a regulator of heritable gene silencing which contributes to both mitotic proliferation as well as sexual commitment of the parasite. PfPPM2 promotes sexual conversion by regulating the interaction between HP1, H3K9me3 and chromatin and it achieves this by dephosphorylating S33 of HP1. PfPPM2 also regulates protein synthesis in the parasite by repressing the phosphorylation of initiation factor eIF2α, which is likely to contribute to parasite division and possibly sexual differentiation.

Malaria continues to be a major public health challenge as it causes ~200 million infections and more than 600,000 deaths each year[1]. *Plasmodium*, the causative agent of malaria, has an unusual life cycle involving morphologically distinct developmental stages. It undergoes asexual division in hepatocytes in the liver followed by asynchronous intraerythrocytic multiplication in the vertebrate host. In each cycle, a small fraction of the asexual parasites convert to nonreplicative sexual gametocytes, which upon ingestion by the mosquito initiate the sexual development[2,3]. Reversible protein phosphorylation mediated by protein kinases and phosphatases are major constituent of signalling pathways and are involved in the development of most organisms. The fact that several of the ~85 kinases and ~27 phosphatases coded by *Plasmodium* genome are indispensable for parasite growth[4,5], reiterates their importance for parasite biology and also suggests that at least some of these may serve as drug targets. The function of several protein phosphatases remains unknown in *P. falciparum* and the organization of parasite signalling pathways is poorly understood.

Present studies are related to protein phosphatase PfPPM2 from human malaria parasite *Plasmodium falciparum*, which belongs to PPM2 family of phosphatases[5]. PfPPM2 is refractory to gene disruption in *P. falciparum* suggesting that it is indispensable for asexual blood stage development of the parasite[6,7]. While its *P.berghei* homologue PbPPM2 was found to be dispensable for the asexual development of the rodent parasite, its disruption resulted in slow growth of parasites. PbPPM2 plays a major role in gametocyte sex allocation and ookinete differentiation[5,8]. However, the underlying mechanisms have remained unclear. We demonstrate that PfPPM2 is involved in asexual division of *Plasmodium falciparum* and it also regulates sexual differentiation of

[1]Eukaryotic Gene Expression Laboratory, National Institute of Immunology, Aruna Asaf Ali Marg, New Delhi, India. [2]Center for Systems Biology and Molecular Medicine [an ICMR Collaborating Centre of Excellence 2024 (ICMR-CCoE 2024)], Yenepoya Research Centre, Yenepoya (Deemed to be University), Mangalore 575018, India. [3]Immunoinformatics Laboratory, National Institute of Immunology, New Delhi, India. [4]Indian Institute of Science Education and Research, Pashan, Pune, Maharashtra 411008, India. e-mail: pushkar@nii.ac.in

this parasite. Detailed investigations revealed that it may control these processes by regulating the phosphorylation of key proteins involved in chromatin remodelling as well as protein translation. Heterochromatin Protein 1 (HP1) was identified as one of its key targets, which was relevant for both asexual division and sexual differentiation of the parasite. In addition, PfPPM2 regulates protein synthesis by regulating eIF2α phosphorylation by eIF2α-kinase PfPK4.

Results

PfPPM2 regulates asexual division of *P. falciparum*

PfPPM2 belongs to Metal Dependent Protein Phosphatase (PPM) family that are regulated by Mg^{2+} and Mn^{2+} [9]. PfPPM2 was proposed to have two phosphatase domains[10]. However, a subsequent study suggested that it has a single catalytic domain which is interrupted by a linker and it also has a putative N-terminal myristoylation signal[5,9]. Given PfPPM2 is refractory to gene disruption[6], an inducible/conditional knockdown approach involving autocatalytic glucosamine (GlcN) regulatable glmS-ribozyme[11] was used. To this end, glmS ribozyme coding sequence was introduced in the PfPPM2 3′-UTR along with a 3xHA tag (Fig. 1A, Supplementary Fig. 1) in 3D7 (PfPPM2-HA-glmS^{3D7}) as well as NF54 (PfPPM2-HA-glmS^{NF54}) background. The treatment of PfPPM2-HA-glmS parasites with GlcN effectively depleted PfPPM2 protein (Fig. 1B). Parasite growth rate assays were performed in which glucosamine (GlcN) was added at early ring stages (cycle 0) and parasite development was monitored periodically for at least two subsequent cycles. A marked decrease in parasitemia was observed at the end of the first cycle, which was even more accentuated in the second cycle (Fig. 1C). The presence of GlcN itself did not affect the asexual proliferation in either 3D7 or NF54 parasite lines (Supplementary Fig. 2A and B). The analysis of Giemsa-stained thin blood smears did not reveal any obvious morphological changes in the parasite, which was also indicated by similar distribution of various developmental stages in PfPPM2-depleted parasites (Supplementary Fig. 2C). Therefore, the decrease in parasitemia was mainly due to a decrease in the number of rings formed at the beginning of cycle 1 and 2. Further analysis revealed that PfPPM2 depletion led to a significant reduction in the number of merozoites formed per schizont (Fig. 1D), which accounted for defects in parasite growth. Independent invasion assays were also performed to assess if the ability of re-invasion was affected but no significant defects in invasion were observed (Supplementary Fig. 2D). Therefore, the decrease in the number of rings was mainly due to lesser number of merozoites formed in PfPPM2-depleted parasites. Collectively, these data suggested a major role of PfPPM2 in parasite division. Immunofluorescence assays (IFA) revealed that PfPPM2 is present in punctate structures near the parasite nucleus during schizogony (Supplementary Fig. 3A), particularly in mid to late schizonts, with some presence in the cytoplasm. In order to gain better insights into the localization of PfPPM2, Ultrastructure Expansion Microscopy (U-ExM) was performed. U-ExM revealed that PfPPM2 localizes in punctate structures, which were often present at or near the nucleus. In addition, PfPPM2 was also found in parasite cytoplasm suggested by smaller puncta especially early in division (Fig. 1E, Supplementary Movie 1 and 2).

To further evaluate the underlying reasons for defects in parasite division, the status of centrosome or centriolar plaque (CP)-which represents the microtubule organization centre (MTOC) of the parasite and spindle formation was determined by staining with anti-centrin and anti-α-tubulin antibody[12]. PfPPM2 depletion revealed parasites with diffused tubulin staining indicative of loss of spindles (Supplementary Fig. 3B). In addition, there was a modest but significant defect in CP duplication (Supplementary Fig. 3C). The defects in spindle formation were more apparent upon analysis by U-ExM, which revealed the formation of hemispindles or mitotic spindles in control parasites. Most PfPPM2 depleted parasites exhibited fragmented tubulin staining indicative of a loss of spindles and only a very few merozoites/nuclei with associated mitotic spindle were observed (Fig. 1F, Supplementary Fig. 3B). Collectively, these results indicated a role of PfPPM2 in asexual division of the parasite, which may be due to its direct or indirect involvement in the above-mentioned processes.

In addition, the formation of inner membrane complex (IMC) was assessed by IMC1g (Supplementary Fig. 3D) or GAP45 (Supplementary Fig. 3E) staining- which is formed during division and speculated to support this process[13], was also disrupted and may be a consequence of arrested nuclear division (Supplementary Fig. 3D,E). Despite disruption in IMC formation, the lack of defects in invasion of PfPPM2 were surprising. Since there are a significant number of merozoites with normal GAP45 and IMC1g staining, it is possible that there were enough number of invasion-competent merozoites with intact IMC/glideosome, which resulted in no significant defects in invasion upon PfPPM2-depletion. Recent studies revealed that IMC1g-depleted parasites which have impaired IMC formation also do not show significant changes in egress and invasion[14,15].

Identification of PfPPM2 targets by phosphoproteomics

Having established the role of PfPPM2 in parasite division, efforts were made to assess the mechanisms via which it may regulate this process, for which it was important to identify its targets or substrates in the parasite. For this purpose, a comparative phosphoproteomic approach was used (Supplementary Fig. 4) to compare the phosphoproteome of parasites after PfPPM2-depletion. Since a major defect was found in parasite division, schizonts (~ 38-40 hpi, 1st cycle) that were left untreated or treated with GlcN were used for this purpose (Supplementary Fig. 4). Overall, 95 phosphosites on 61 proteins exhibited enhanced phosphorylation upon phosphatase depletion (Fig. 2A, Supplementary Data 1 and 2). In addition, 35 phosphosites on 27 proteins were identified as hypophosphorylated in the PfPPM2-depleted parasites, which may be due to direct or indirect effects exerted by PfPPM2 on a protein kinase or by negatively regulating other protein phosphatases.

The differentially phosphorylated proteins in PfPPM2 depleted parasites belonged to three major family of proteins (Fig. 2A, Supplementary Data 1 and 2): chromatin remodelling, assembly and related functions (histone H3 and H3 variant 3.3, Heterochromatin Protein 1, ISWI chromatin remodelling complex ATPase); protein translation (eukaryotic translation initiation factor 2-alpha kinase, elongation factor 1-α,); IMC formation [(basal complex transmembrane protein 1/2 (BTP1/2)], CINCH (Supplementary Table 1). Interestingly, each of these processes can affect parasite division, which as mentioned above is regulated by PfPPM2. For instance, both protein synthesis[16] and chromatin organization are critical for cell division. Epigenetic factors involved in chromatin organization and remodelling are known to be critical for the tight regulation and timely expression of genes in *P. falciparum*. IMC formation has been implicated in the division of Apicomplexan parasites *Toxoplasma* and *Plasmodium*[13,17]. As mentioned above, PfPPM2 depletion impaired IMC biogenesis (Supplementary Fig. 3D,E), which may be due to altered phosphorylation of the above-mentioned proteins. Since PfPPM2 was not localized to the IMC, it is possible that it may not directly regulate IMC biogenesis; instead, it may be an outcome of arrest in parasite division.

PfPPM2 may regulate epigenetic regulators and components of translation machinery. Since both phosphoproteomics (Fig. 2A, Supplementary Table 1 and Data 1 and 2) and transcriptomics (Supplementary Fig. 9, discussed below) indicated that PfPPM2 may regulate genes/proteins involved in translation, its role in protein synthesis was assessed. Interestingly, phosphoproteomics data suggested that PfPPM2 may regulate the phosphorylation of eIF2α-kinase PfPK4 as two residues (S1773, S1973) were found to be hyperphosphorylated upon PfPPM2 depletion (Fig. 2A, Supplementary Table 1, Supplementary Fig. 5A). In the case of malaria parasite,

https://doi.org/10.1038/s41467-025-59476-w

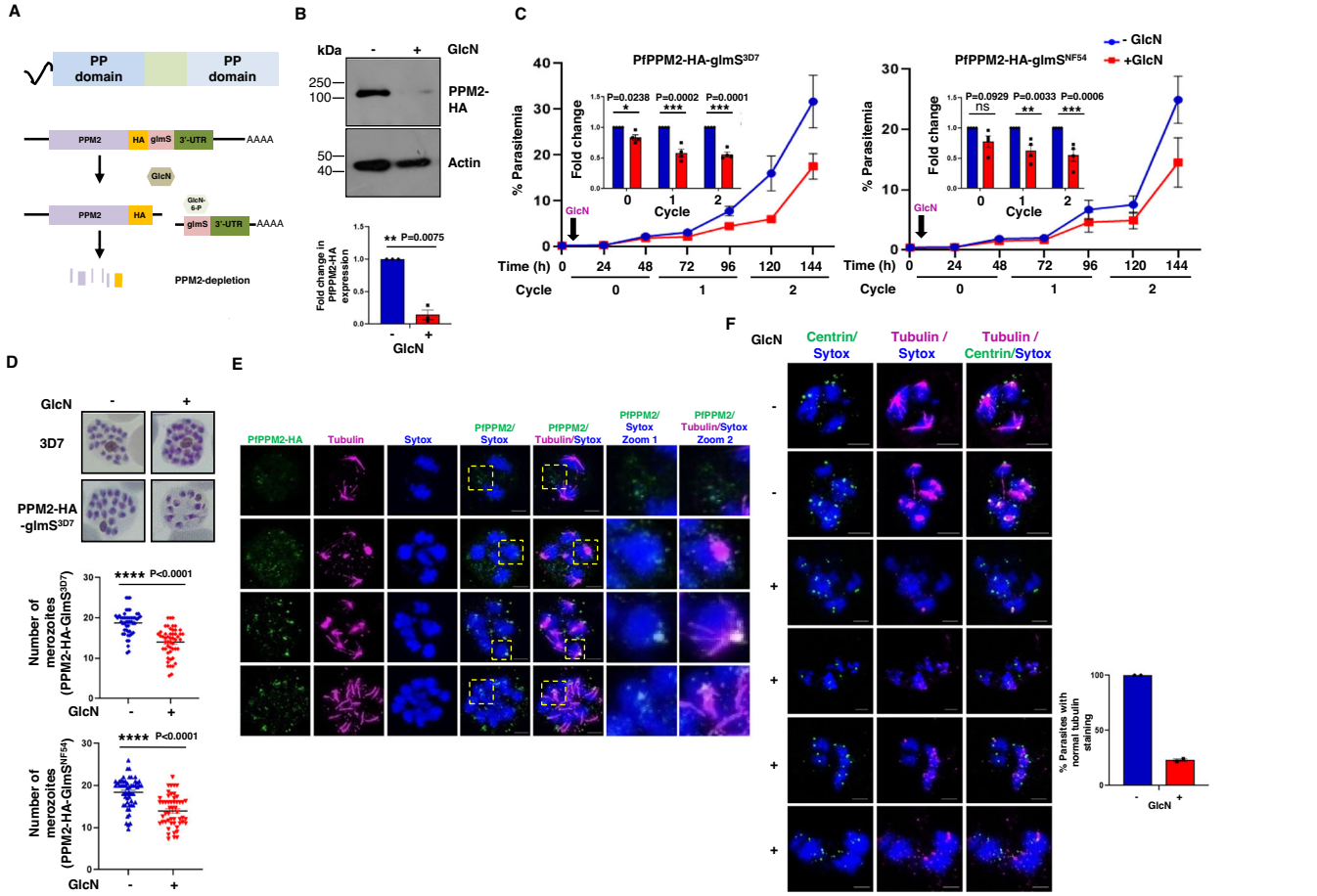

Fig. 1 | PfPPM2 regulates asexual division of *Plasmodium falciparum*. **A** PfPPM2 has an insert between its PP domain and also has a putative N-terminal myristylation signal[5,56]. In order to achieve conditional knockdown (cKD) of *PfPPM2*, a ribozyme glmS was introduced at its 3'end along with a HA-tag in 3D7 as well as NF54 background (Supplementary Fig. 1). The addition of glucosamine and subsequent conversion to GlcN6P activates the ribozyme and will result in its cleavage and degradation of the mRNA causing depletion of PfPPM2 protein. **B** Western blotting of PfPPM2-HA-glmS^{3D7} parasites, which were either left untreated or treated with GlcN (cycle 0, rings) and parasite lysates were prepared (schizonts, cycle 1) using anti-HA antibody, which caused effective depletion of PfPPM2-HA. β-actin antibody was also used to probe the blots. *Bottom Panel*, Fold change in PfPPM2 depletion was determined by densitometry of PfPPM2 bands in the Western blots, which was normalized with respect to actin (Statistical differences were determined using paired Two-tailed Student's t-tests, $^{**}P < 0.01$. Single data points and mean ± SEM of three biological replicates are shown). **C** PfPPM2-HA-glmS^{3D7}(left panel) or PfPPM2-HA-glmS^{NF54} (right panel) parasites were synchronized and ring stage parasites were used for setting up growth rate assay in the presence or absence of GlcN. Parasite growth was assessed after each cycle by performing flow cytometry (right panel) as well as analysis and counting parasites from Giemsa-stained smears (left panel). *Inset*, fold change in parasitemia of GlcN treated with respect to untreated parasites was determined (Statistical differences were determined using Two-way ANOVA, $^{*}P < 0.05$, $^{**}P < 0.01$, $^{***}P < 0.001$. Single data points and mean ± SEM of four biological replicates are shown). The arrow indicates the time of GlcN-addition. **D** PfPPM2-HA-glmS$^{3D7/NF54}$ parasites were treated with GlcN as described in panel **B**. Thin blood smears were made at ~40–44 hpi in cycle 1. The numbers of nuclear centers/merozoites were counted from Giemsa-stained thin blood smears. (Statistical analysis was performed using unpaired Two-tailed Welch's t-tests, $^{****}P < 0.0001$, $n > 120$ schizonts were counted in each condition. Each point represents a schizont and mean ± SEM of three biological replicates are shown). **E** PfPPM2-HA-glmS^{NF54} parasites were synchronized and U-ExM was performed on schizonts during various stages of division (~ 36-44 h.p.i) using anti-HA and anti-tubulin antibody. The localization of PfPPM2-HA was mainly cytoplasmic early in division. However, in more mature schizonts it was frequently localized as puncta close to the nucleus. Scale bar =5 µm. A zoomed projection of individual merozoites is also provided. A projection of z-sections of images in rows 3 and 4 is also provided as videos in Supplement (Supplementary Movie 1 and 2). **F** PfPPM2-HA-glmS^{NF54} parasites were treated with GlcN as described in panel **B** and **C**. U-ExM was performed on schizonts (cycle 1) using anti-tubulin and anti-centrin antibodies which revealed the presence of hemispindles, mitotic spindles and interpolar spindles in untreated parasites. GlcN treatment resulted in a loss of spindles in most parasites. Scale bar = 5 µm. *Right Panel*, percent parasites with normal tubulin staining- reflected by the presence of above-mentioned forms of spindles- were counted from U-ExM images (total number of parasites counted = 65 each in control and knockdown condition). The images for quantification were acquired from two independent experiments. Data is plotted as mean ± SEM of two biological replicates. Source data are provided as a Source Data file.

protein kinase PK4 has been implicated in eIF2α phosphorylation at S59, which prevents protein synthesis (Supplementary Fig. 5B)[18]. Western blotting was performed using anti-phospho-eIF2α antibody, which recognizes the complementary site (S59) on its *Plasmodium* homologue[18,19]. PfPPM2 depletion resulted in a dramatic increase in eIF2α phosphorylation (Supplementary Fig. 5C) suggesting that PfPPM2 normally suppresses this during asexual development. Given that phosphorylation of eIF2α at this site is critical for the regulation of protein translation in several organisms including *Plasmodium*[18,19], changes in protein synthesis were assessed. To this end, puromycin incorporation assays were performed to assess the status of protein synthesis[20,21]. Strikingly, PfPPM2 depletion caused a marked reduction in puromycin incorporation in schizonts but not in trophozoites, which was suggestive of impaired protein synthesis (Supplementary Fig. 5D) that coincided with defects in parasite division. Therefore, PfPPM2 may directly or indirectly regulate PK4 activity and/or dephosphorylate eIF2α at this site to promote protein synthesis during parasite division.

https://doi.org/10.1038/s41467-025-59476-w

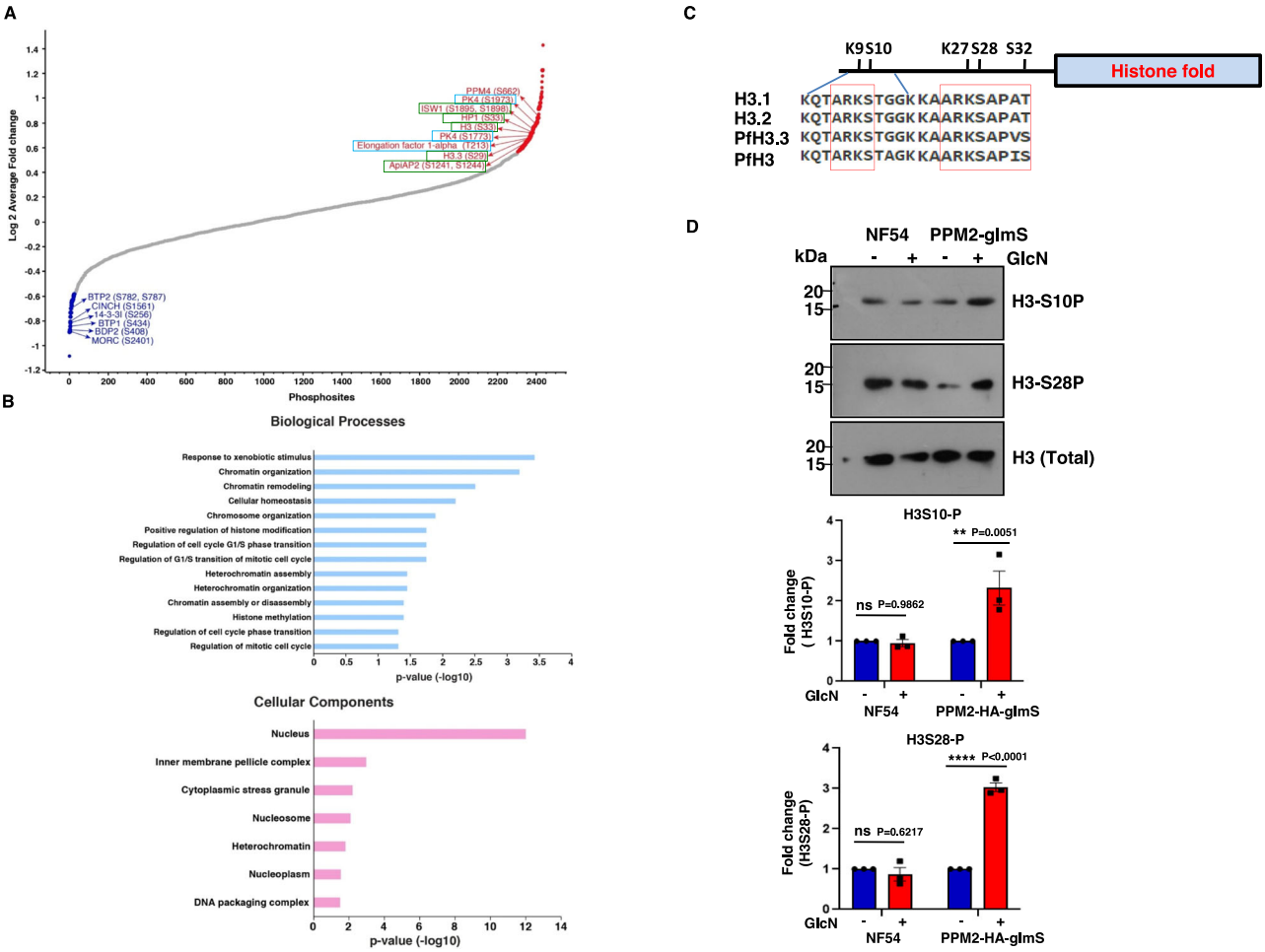

Fig. 2 | PfPPM2 regulates the phosphorylation of key parasite proteins involved in chromatin remodelling and translation. A PfPPM2-HA-glmS^{3D7} parasites were treated with GlcN as described in Fig. 1B and C to perform comparative phosphoproteomic and proteomic analyses as indicated in the schematic (Supplementary Fig. 4). The S-curve represents fold-change ratios of identified phosphopeptides upon GlcN treatment (Supplementary Data 1.1). Some of the significantly altered phosphorylation sites (red and blue) belonging to key proteins relevant for protein synthesis or chromatin organisation (Supplementary Data 1.2, 1.3) are outlined in cyan and green, respectively. **B** Gene Ontology enrichment of proteins that exhibited significant changes in phosphorylation upon PfPPM2 depletion (Supplementary Data 1.5, 1.6). The phosphorylation fold-change ratio of identified phosphopeptides was normalized to total protein abundance fold-change. A one-sample, two-sided Student's t-test was performed on the normalized values from three biological replicates ($n = 3$) to identify proteins with significant deviations. Pathways are represented based on their $-\log_{10}$(P values), as estimated by the Gene Ontology tool available at PlasmoDB. **C** Sequence comparison of N-terminal tail of human histone H3 variants with *P. falciparum* Histone H3 and H3.3. Key motifs containing regulatory sites indicated by red square and critical residues that are modified by phosphorylation (S10, S28, S32), methylation (K9) and acetylation (K9, K27) are indicated. **D** Western blot analysis using specific antibodies against pS10-H3, pS28-H3 performed on NF54 and PfPPM2-HA-glmS^{NF54} lines cultured in the absence and presence of GlcN. *Lower Panel*, densitometry analysis was performed and fold change in GlcN-treated parasites compared to untreated parasites was determined. (Statistical differences were determined using Two-way ANOVA, ** $p < 0.01$,**** $p < 0.0001$, $P > 0.05$,ns-nonsignificant. Single data points and mean ± SEM of three biological replicates are shown). Source data are provided as a Source Data file.

One of the highlights of phosphoproteomic studies was the aberrant phosphorylation of several proteins involved in chromatin remodelling, which included HP1, Histone H3 and its variant H3.3 in PfPPM2-depleted parasites (Fig. 2A, Supplementary Table 1, Data 1 and 2). Histone H3 and its variant H3.3 were found to be hyperphopshorylated at S33 and S29 (corresponding to S28 on histone H3), respectively. Since S29 is equivalent to S28 of histone H3 and H3.3 homologues of most species, it will be hereafter referred to as S28[22]. In the case of mammalian cells, phosphorylation of S28 is very well known for its role in mitosis and can act as a distinctive mark for dividing cells[23–25]. Although a phosphopeptide with phospho-S10 H3 was not detected, it is also known to be critical for cell division. Since these sites are very well conserved in PfHistone H3 and its variant H3.3 (Fig. 2C), it is very likely that the phosphorylation of these sites is important for a similar function in the malaria parasite. Therefore, the role of PfPPM2 in S10 and S28 H3 phosphorylation was assessed using specific commercial phospho-S10/S28 antibodies. Strikingly, the phosphorylation of both these sites was significantly enhanced upon PfPPM2 depletion (Fig. 2D), which confirmed findings from the phosphoproteomics analysis (Supplementary Table 1, Data 1 and 2) and implicated a possible direct or indirect role of PfPPM2 in the dephosphorylation of these sites. Previous studies performed on mammalian cells have indicated that dephosphorylation of these and other sites on Histone H3 is critical before cells exit the M-phase failing which they undergo arrest[24]. Therefore, it is possible that PfPPM2 mediated dephosphorylation of Histone H3 contributes to parasite division in concert with other chromatin remodelling proteins indicated above.

Since the aberrant phosphorylation of histone H3 and other epigenetic regulators is likely to impact gene expression, it was pertinent to assess changes in parasite transcriptome upon PfPPM2 depletion. RNA-sequencing (RNA-Seq) analysis of PfPPM2-HA-glmS^{NF54} parasites

at schizont stage revealed several genes that exhibited altered expression upon PfPPM2 depletion (Supplementary Fig. 9A and Supplementary Data 3). Gene Set Enrichment Analysis (GSEA) using ClusterProfiler[26] highlighted significant enrichment of Gene Ontology (GO) terms involved in translation as well as cell division (Supplementary Fig. 9B). For instance, two centrins (Centrin 4 and Centrin 1), PCNA and MCM3- were downregulated in PfPPM2-depleted parasites (Supplementary Fig. 9, Data 3), which fits in well with defects in MTOC/CP duplication and division of these parasites (Fig. 1F, Supplementary Fig. 3B,C). Additionally, several genes involved in translation showed altered expression (Supplementary Fig. 9). This is particularly noteworthy as phosphoproteomics also revealed that numerous key proteins associated with translation displayed changes in phosphorylation upon PfPPM2 depletion (Fig. 2A,B, Supplementary Table 1). Importantly, as described above, PfPPM2 indeed regulates protein synthesis by suppressing the phosphorylation of eIF2α. Given that both chromatin remodelling and protein synthesis regulate cell division, these results provided first insights into the mechanisms by which PfPPM2 may regulate parasite division.

PfPPM2 regulates HP1, which is essential for sexual differentiation and asexual development

PfHP1 is a heterochromatic protein that maintains heterochromatin structure and plays roles in var gene silencing, sexual differentiation, and asexual development of the parasite[27–30]. Phosphoproteomics analysis revealed that S33 present in the chromodomain (CD) of PfHP1 was hyperphosphorylated upon PfPPM2 depletion. While this phosphorylation site is conserved in human HP1 homologues, it is replaced by an aspartic acid residue in *S. pombe* Swi6 (Fig. 3A). Western blot using an custom antibody, generated against a phosphopeptide containing the sequence encompassing phospho-S33 (pS33-HP1), also revealed that phosphorylation of S33 was significantly enhanced upon PfPPM2 depletion, supporting phosphoproteomics data and suggesting that PfPPM2 may dephosphorylate this site on HP1 (Fig. 3B).

PfHP1 is known to regulate gametocytogenesis or sexual differentiation[27]. Given PfPPM2 contributes to its dephosphoryation (Fig. 2A, Supplementary Table 1, Data 1 and 2), we examined if PfPPM2 had a role to play in sexual conversion or gametocyte formation. For this purpose, gametocyte formation of PfPPM2-HA-glmS^{NF54} parasites was assessed, which was induced by the addition of serum free media and treatment with N-acetyl glucosamine (NAG) was provided to kill asexual forms[31]. While there was no difference in the case of parental NF54 line, a significant reduction in parasite sexual conversion in PfPPM2-HA-glmS^{NF54} parasites was observed upon PfPPM2 depletion (Fig. 3C). These data were consistent with studies performed in *P. berghei*, which implicated PPM2 in gametocyte formation[5]. The transcription factor AP2-G is a master regulator of sexual commitment, which is kept repressed by HP1 and H3K9me3[29,32], and induction of its expression is critical for the conversion of asexual to sexual forms[33]. AP2-G expression was determined at the schizont stage by qRT-PCR, which revealed that PfPPM2 depletion significantly reduced AP2-G expression (Fig. 3D) and corroborated well with impaired sexual conversion (Fig. 3C).

HP1 associated H3K9me3 occupies the heterochromatin regions and represses the expression of heterochromatic genes. PfAP2-G is one of the few euchromatic genes that are silenced by HP1-H3K9me3, which is critical for sexual commitment[27]. The impact of PfPPM2 depletion on HP1 and H3K9me3 at the promoter of AP2-G was assessed by ChIP-qPCR at the schizont stage[27]. Results from these assays revealed that PfPPM2 depletion caused a significant increase in both HP1 as well as H3K9me3 occupancy at AP2-G loci (Fig. 3E). Occupancy on gametocyte specific gene Pfs16, which was used as a control and is not regulated by HP1 or H3K9me3, did not show any difference. Furthermore, Western blot was also performed to check the levels of H3K9me3 in the case of PfPPM2 depletion. A significant increase in H3K9me3 was also observed under PfPPM2 depletion (Fig. 3F), which is likely to enhance HP1 deposition on the genome and formation of heterochromatin[34]. These observations suggested that PfPPM2 may promote AP2-G expression by deregulating the interaction of HP1 and H3K9me3 with its promoter during sexual differentiation.

Collectively, these observations indicated that the regulation of HP1 by PfPPM2 is important for AP2-G derepression and sexual differentiation of the parasite.

Optimal HP1-S33 phosphorylation levels are critical for asexual development and sexual differentiation of the parasite

The possibility of PfPPM2 mediated regulation of HP1 playing a role in asexual development of the parasites was also investigated. For this purpose, HP1 was episomally expressed in PfPPM2-HA-glmS^{NF54} parasites (PfPPM2-HA-glmS^{NF54}:HP1-GFP^{OE}) (Supplementary Fig. 6A,B). Growth rate assays revealed that HP1 overexpression significantly reversed the defects in parasite growth that were observed upon PfPPM2 depletion (Fig. 4A). In addition, parasite division-indicated by the number of merozoites or nuclear centers per schizonts which is impaired in PfPPM2-HA-glmS^{NF54} parasites was also significantly restored (Fig. 4B). HP1 overexpression also reverted the impaired gametocyte formation as a result of PfPPM2-depletion (Supplementary Fig. 6C). These data suggested that constitutive overexpression of HP1 was able to significantly revert the defects observed in PfPPM2 depleted parasites.

Next, we attempted to mutate the PfPPM2-target site in the endogenous HP1 locus to generate S33 phosphodeficient (S33A) and phosphomimetic mutants (S33D). These efforts yielded a mixed population that contained parasites with S33A mutation along with wild type unmodified HP1 (Supplementary Fig. 7) (PfPPM2-3xHA-GlmS$^{NF54:HP1/HP1-S33A-Flag}$), which could be distinguished by IFA with anti-Flag antibody. We were unable to generate S33D mutant parasites which could be due to deleterious effects of this mutation. The flag-tagged HP1-S33A parasites were extremely slow growing and possessed gametocyte-like morphology. IFA revealed that ~60% of S33A mutant Flag-tagged parasites were gametocytes as they expressed gametocyte specific protein Pfs16. In contrast, most WT HP1-Flag parasites remained asexual (Fig. 4C). These data were consistent with the fact that PfPPM2 mediated dephosphorylation at S33 of HP1 may promote sexual conversion of the parasite.

To evaluate this further, we attempted episomal overexpression of HP1 S33A and S33D mutants in PfPPM2-HA-glmS^{NF54} parasites. Since multiple attempts to either episomally express S33A or S33D mutants were unsuccessful, HP1 phosphomutants tagged with GFP were conditionally overexpressed in NF54 parasite line by fusing with the FKBP Death Domain (DD) at its C-terminus (Supplementary Fig. 8A), which can be stabilized by the addition of Shield-1[35]. Western blotting revealed successful over-expression of the recombinant proteins (HP1/S33A/S33D-GFP-DD) in the presence of Shld-1 but some amount of proteins was also expressed in its absence and was indicative of “leaky” expression (Supplementary Fig. 8B). Growth rate assays revealed that both S33A and S33D mutant expressing parasites impaired asexual development as the parasitemia for these parasite lines did not increase and was much lower in cycles 1 and 2 in comparison to WT-HP1 expressing parasites (Fig. 5A). Since these defects were observed in the absence of Shld-1, even low levels of these mutant proteins seemed to impair asexual parasite development.

The analysis of S33D mutant, which represents S33 hyperphosphorylated form of HP1, overexpressing parasites revealed arrested development as only a small population of trophozoites progressed to schizonts and a significant number of parasites exhibited

https://doi.org/10.1038/s41467-025-59476-w

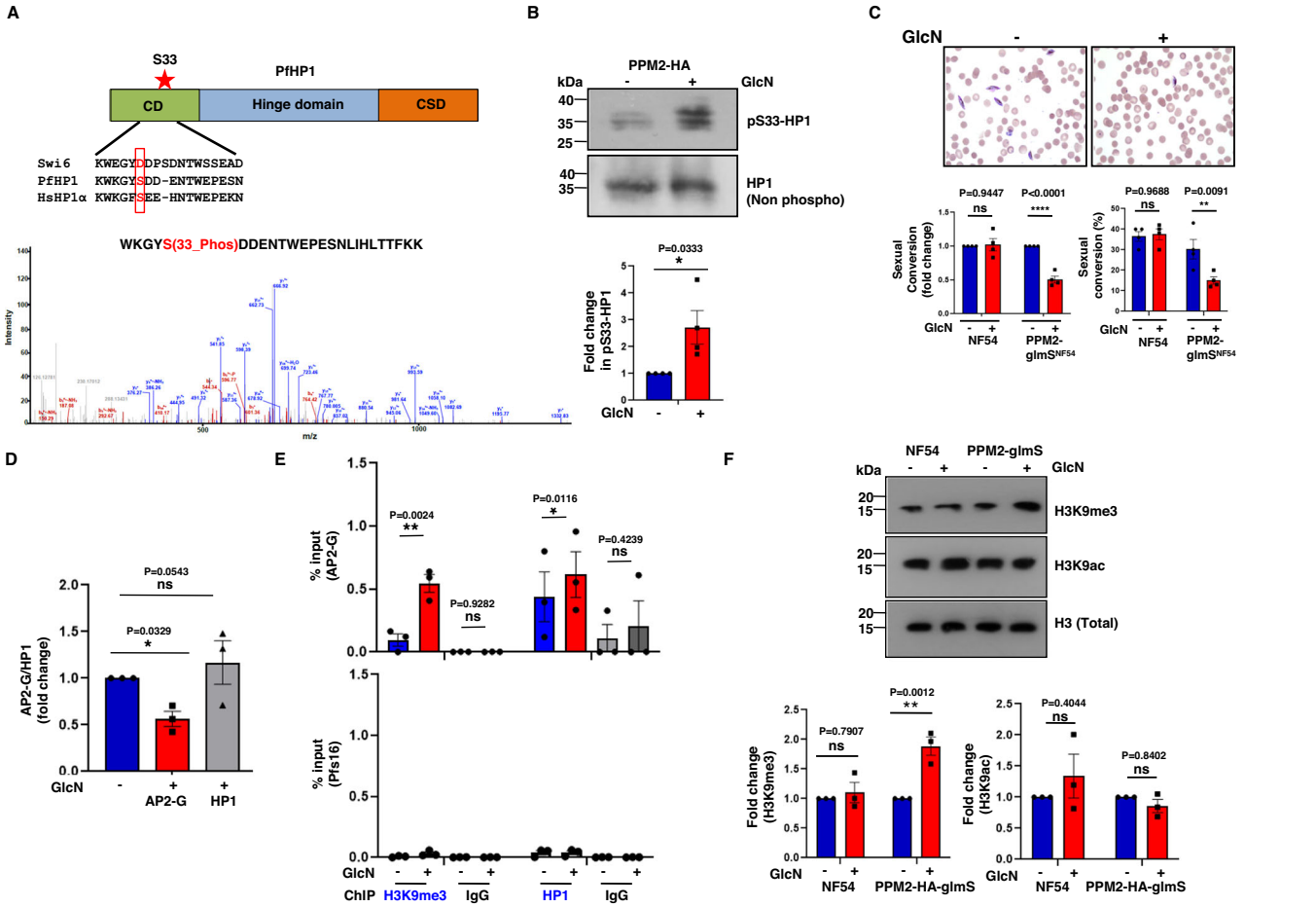

Fig. 3 | PfPPM2 regulates HP1 phosphorylation and sexual conversion of the parasite. A. PfPPM2 depletion causes hyperphosphorylation of S33 (*) present in its chromodomain (CD). S33 seems to be conserved in human HP1α and HP1β (not shown here) and is replaced by a D in *S. pombe* homologue swi6. *Bottom panel*, MS/MS spectra for peptide corresponding to pS33-HP1. **B** Western blotting of lysates from PfPPM2-HA-glmS^{NF54} parasites, which were either left untreated or treated with GlcN using antibody against pS33-HP1 (see methods for details) or its phosphorylation-independent version. *Bottom Panel*, Fold change in HP1-S33 phosphorylation upon PfPPM2 depletion in experiments described in the upper panel was determined by densitometry (Statistical differences were determined using unpaired Two-tailed Student's t-tests, $^{*}P < 0.05$. Single data points and mean ± SEM of four biological replicates are shown). **C** PfPPM2-HA-glmS^{NF54} or NF54 (control) parasites were cultured in the presence or absence of GlcN and gametocyte formation was induced as described in Methods. The number of gametocytes formed after GlcN-treatment was counted and fold change in sexual conversion and % conversion of asexual parasites to gametocytes was determined at day 5 p.g.i. (Statistical analysis was performed using Two-way ANOVA, **** $p < 0.0001$; $^{**}P < 0.01$, ns $p > 0.05$. Single data points and mean ± SEM of four biological replicates are shown). **D** Gametocyte formation was induced in GlcN-treated or untreated PfPPM2-HA-glmS^{NF54} parasite. qRT-PCR was performed after 24 h of gametocyte induction to compare the expression of AP2-G and HP1 (Statistical analysis was performed using paired Two-tailed Student's t-tests, $^{*}p < 0.05$, ns $p > 0.05$). Single data points and mean ± SEM of three biological replicates are shown). **E** ChIP-qPCR was performed to determine PfHP1 and H3K9me3 occupancy at AP2-G or Pfs16 loci in PfPPM2-HA-glmS^{NF54} parasites which were either left untreated or treated with GlcN. IgG antibody was used for ChIP as a negative control (Statistical analysis was performed using paired Two-tailed Student's t-tests, $^{**}P < 0.01$, $^{*}p < 0.05$, ns $p > 0.05$. Single data points and mean ± SEM of three biological replicates are shown). **F** Western blotting of lysates from PfPPM2-HA-glmS^{NF54} or NF54 parasites, which were either left untreated or treated with GlcN using antibodies against H3K9me3, H3K9ac or total H3. *Bottom Panel*, Fold change in H3K9me3 and H3K9ac upon PfPPM2 depletion in experiments described in the above panel was determined by densitometry (Statistical analysis was performed using Two-way ANOVA, $^{**}P < 0.01$, ns $p > 0.05$. Single data points and mean ± SEM of three biological replicates are shown). Source data are provided as a Source Data file.

abnormal pyknotic morphology (Fig. 5B). These data suggested that S33D mutant causes cell cycle arrest and is possibly toxic to the parasites. In contrast, the majority of the S33A-overexpressing parasites had gametocytes like morphology (Fig. 5B), which was confirmed with IFA using antibodies against gametocyte specific protein Pfs16 (Fig. 5C). While only a small fraction of WT-HP1 and S33D overexpressing parasites exhibited Pfs16 staining, in the case of S33A, ~ 60% GFP+ cells were Pfs16 + . Moreover, these gametocytes developed further to stage IV-V after six days (Fig. 5C). These data confirmed that S33A mutation results in gametocyte formation, which explained slow growth rates of the S33A-overexpressing parasites (Fig. 5A). qRT-PCR revealed that the expression of AP2-G as well as Pfs16 was significantly higher in S33A mutant overexpressing parasites (Fig. 5D), which corroborated well with the fact that these parasites were mainly gametocytes. Collectively, these data suggested that dephosphorylation of HP1 at S33 by PfPPM2 activation- which is mimicked by the S33A mutant-promotes sexual differentiation of the parasite and PfPPM2 depletion prevents this process. While phosphorylation of HP1-S33 is critical for parasite asexual divsion, its hyperphosphorylation mimicked by S33D mutant, which to some extent represents PfPPM2-depleted state, can cause arrest in parasite development.

Next, using the S33A/D mutants, efforts were made to investigate if S33 dephosphorylation regulates HP1-H3K9me3 interaction. To this end, immunoprecipitation was performed to assess the interaction between WT or mutant HP1 with H3K9me3 using these transgenic

https://doi.org/10.1038/s41467-025-59476-w

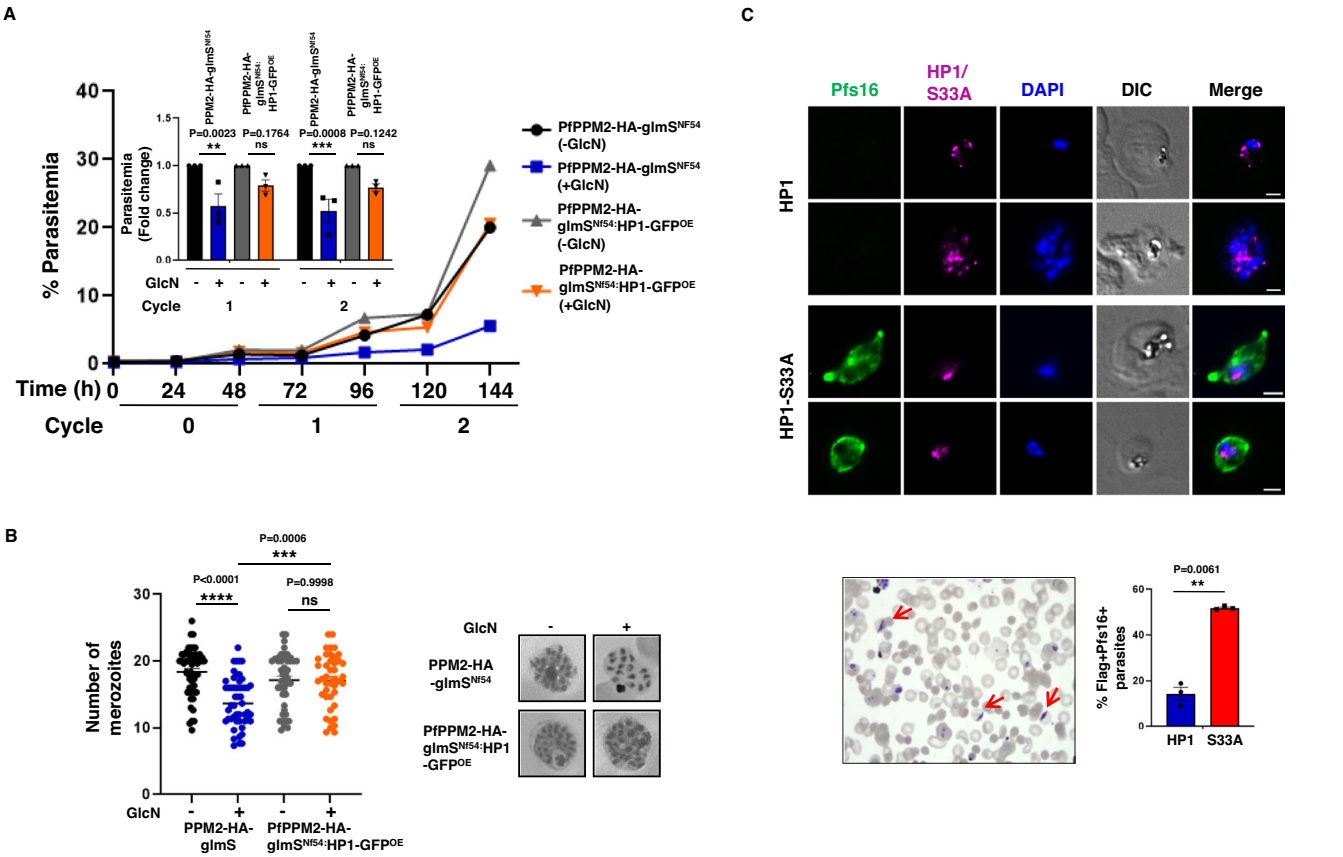

Fig. 4 | PfPPM2 mediated HP1 phosphorylation may be critical for asexual development and sexual differentiation. A PfPPM2-HA-GlmS^{NF54} parasites or HP1-GFP overexpressing PfPPM2-HA-glmS^{Nf54}:HP1-GFP^{OE} parasites were synchronized, treated with GlcN (cycle 0) and growth rate assays were performed to determine the parasitemia by flow cytometry as described for Fig. 1C. *Inset*, fold change in parasitemia was determined with respect to untreated parasites in the next two cycles (Statistical analysis was performed using Two-way ANOVA, $^{**}P < 0.01$, $^{***}P < 0.001$, $P > 0.05$, ns-non-significant. Single data points and mean ± SEM of three biological replicates are shown). **B** PfPPM2-HA-GlmS^{NF54} or PfPPM2-HA-glmS^{Nf54}:HP1-GFP^{OE} parasites were treated with GlcN as described in panel A. Thin blood smears were made ~40–44 hpi in cycle 1. The number of nuclear centers/ merozoites were counted from Giemsa-stained thin blood smears. (Statistical analysis was performed using one-way ANOVA, $^{****}P < 0.0001$, $^{***}P < 0.001$, ns-nonsignificant, $n > 100$ schizonts were counted in each condition and each data point represents a schizont. Mean ± SEM of three biological replicates are shown). **C** IFA was performed on PfPPM2-3xHA-GlmS$^{NF54:HP1/HP1-S33A-Flag}$ parasites in which WT-HP1 or its S33A mutant (Supplementary Fig. 7) were tagged with Flag. Anti-Flag antibody was used to detect parasites with tagged proteins and anti-Pfs16 was used to stain gametocytes. Scale bar =2 µm. A representative image of Giemsa-stained smear of S33A mutant parasites with a significant number of gametocytes (red arrows). *Bottom panel*, % Flag-tagged parasites that exhibited Pfs16 expression in IFA. (Statistical analysis was performed using paired Two-tailed Student's t-test, $^{**}P < 0.01$. $n > 120$ parasites each in WT-HP1 and S33A-HP1 were counted. Single data points and mean ± SEM of three biological replicates are shown). Source data are provided as a Source Data file.

parasites. GFP-HP1 was able to pull down H3K9me3 suggesting an interaction between these proteins, as reported previously[28]. Strikingly, there was a dramatic loss of its interaction upon S33A mutation (Fig. 5E, Supplementary Fig. 10). In contrast, the amount of H3K9me3 pulled down with S33D mutant was almost unaltered. Furthermore, Western blotting of nuclear lysate indicated that levels of H3K9me3 were also reduced in the case of S33A mutant in comparison to WT or S33D overexpressing parasites (Fig. 5E, Supplementary Fig. 10). These data suggested that the dephosphorylation of S33 prevents the interaction of HP1 with H3K9me3 and may also impair trimethylation of H3K9, which results in the expression of AP2-G and sexual differentiation of the parasite. Therefore, dephosphorylation of pS33-HP1 is a signal for sexual commitment. Consistent with this, IFA revealed that most WT-HP1 or S33D overexpressing asexual parasites were stained with anti-pS33-HP1. In contrast, pS33-HP1 was absent from most S33A-overexpressing parasites, which were mainly gametocytes (Fig. 6A). Since S33 was replaced by A or D in the episomal copy, pS33-HP1 staining mainly reflects the phosphorylation status of the endogenous HP1 in these S33A/D parasite lines. Therefore, S33A mutant is dominant and promotes gametocyte formation, which lack S33 phosphorylation (also described below).

Next, the effect of induction of sexual conversion by serum removal on pS33-HP1 levels was assessed (Fig. 6B). IFA revealed that more than half of the PfPPM2-HA-glmS^{NF54} schizonts exhibited pS33-HP1 staining but upon induction of sexual conversion most of the parasites that were either gametocytes and almost all schizonts- possibly sexually committed forms- lost pS33 phosphorylation (Fig. 6B). In contrast, upon PfPPM2 depletion, even after induction, mostly shizonts were observed that exhibited pS33 staining. Given that PfPPM2-depletion prevents sexual differentiation (Fig. 3C), it is reasonable to suggest that these pS33-HP1-positive schizonts are unable to undergo gametocytogenesis due to lack of PfPPM2-mediated dephosphorylation of this site. Furthermore, in an unrelated parasite line, pS33-HP1 staining was also lost upon conversion to gametocytes and was observed mainly in asexual parasites (Supplementary Fig. 11). Collectively, these data suggested that dephosphorylation of S33 of HP1 by PfPPM2 is a signal for sexual differentaition of the parasite, which triggers epigenetic changes necessary for this process (Fig. 6C).

https://doi.org/10.1038/s41467-025-59476-w

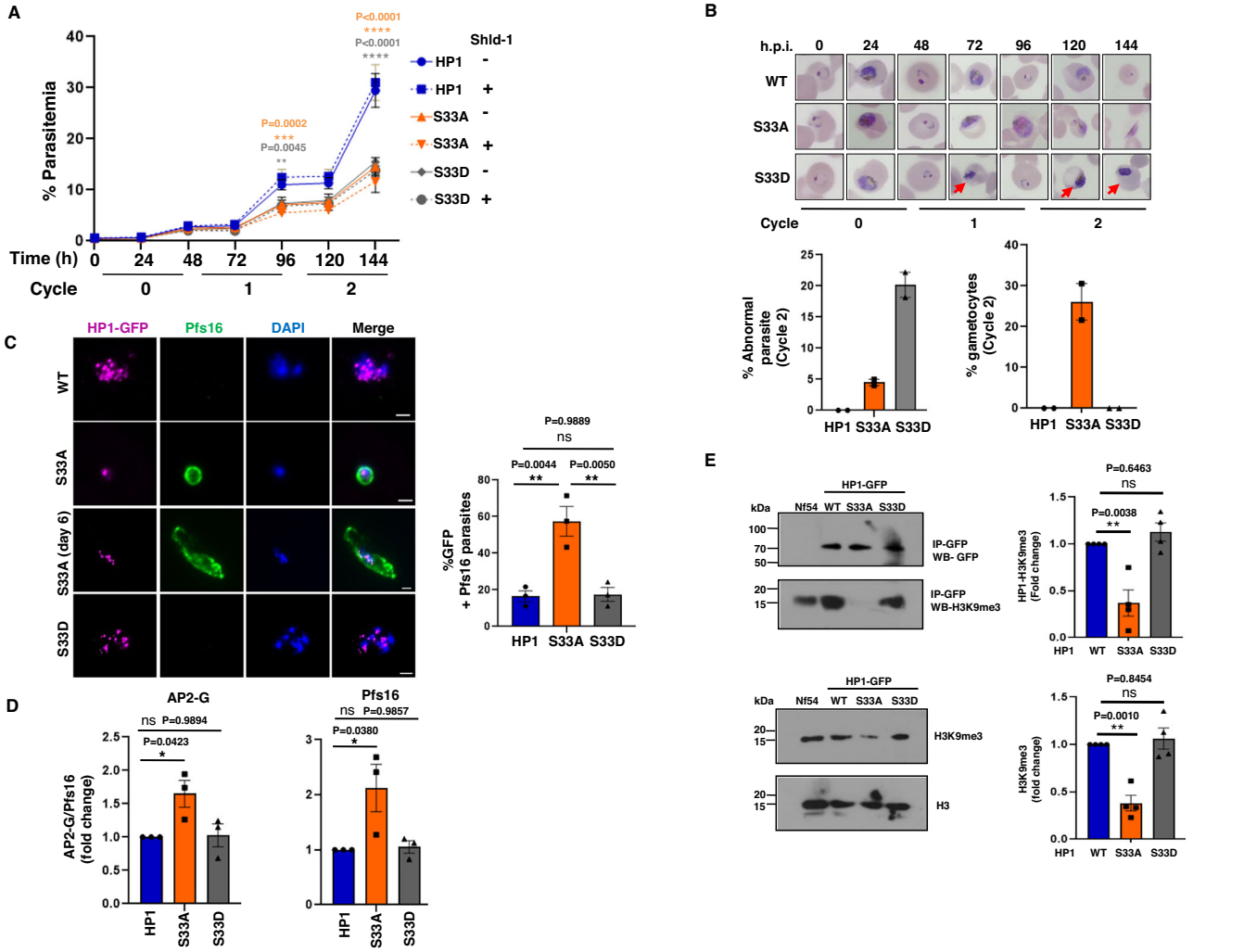

Fig. 5 | Phosphorylation state of HP1 at S33 is critical for asexual and sexual development of *P. falciparum*. **A**. HP1/S33A/S33D-GFP-DD parasites-which were generated by overexpressing HP1 or its S33A/D mutants with a GFP and DD domain (Supplementary Fig. 8A,B) were synchronized and ring stage parasites were used for setting up growth rate assay in the presence or absence of Shld-1. Parasitemia was determined after each cycle at the indicated time points from Giemsa-stained thin blood smears of parasite cultures and are represented as % of total number of parasites (Statistical analysis was performed to compare growth of shld1-treated S33A (orange) and S33D (grey) mutant with that of WT-HP1(blue) over expressing parasites using Two–way ANOVA, $^{**}P < 0.01$, $^{***}P < 0.001$, $^{****}P < 0.0001$. Data are mean ± SEM of three biological replicates). **B** Thin blood smears were made for HP1/S33A/S33D-GFP-DD parasites cultured in the presence of Shld1 at indicated time point and stained with Giemsa to assess their morphology. Gametocytes dominated S33A cultures from cycle 1 and in the case of S33D mutant parasites several parasites exhibited abnormal morphology (red arrows). *Bottom Panel*, % parasites with abnormal or gametocyte morphology was determined. Single data points and mean ± SEM of two biological replicates are shown. **C** IFA was performed on thin blood smears of HP1/S33A/S33D-GFP-DD parasites cultured in the presence of Shld1 using anti-GFP and anti-Pfs16 antibodies. *Right Panel*, % of GFP positive parasites that exhibited Pfs16 staining was determined (Statistical analysis was performed using One-way ANOVA, $^{**}P < 0.01$, ns- $p > 0.05$. $n > 90$ parasites each in HP1/S33A/S33D were counted. Single data points and mean ± SEM of three biological replicates are shown). Scale bar = 2 µm. **D** qRT-PCR was performed on Shld-1 treated HP1/S33A/S33D-GFP-DD parasites in cycle 1 to assess the fold change in AP2-G and Pfs16 expression with respect to WT-HP1 overexpressing parasites (Statistical analysis was performed using One-way ANOVA, $^{*}P < 0.05$, $p > 0.05$ ns-not significant. Single data points and mean ± SEM of three biological replicates are shown). **E**. Nuclear protein lysates prepared from NF54 or HP1/S33A/S33D-GFP-DD parasites cultured in the presence of Shld-1 were used for immunoprecipitation using anti-GFP antibody. The IP (upper panel) or protein lysate (bottom panel) were used for Western blotting using indicated anti-GFP or anti-H3K9me3 and anti-H3 antibodies. *Upper Right Panel*, H3K9me3 co-immunopreciptated with HP1 or S33A/S33D mutants was quantitated by densitometry after normalization with respect to H3K9me3 present in total lysate (*Bottom Panel*). Subsequently, fold change in H3K9me3 present in IP of S33A/S33D mutants with respect to WT HP1 was determined. (Statistical analysis was performed using One-way ANOVA, $^{**}P < 0.01$, $p > 0.05$, ns. Single data points and mean ± SEM of four biological replicates are shown). *Bottom Right Panel*, Fold change in H3K9me3 levels was determined in S33A/D mutants with respect to WT HP1 after normalization with respect to total H3 (Statistical analysis was performed using One-way ANOVA,$^{**}P < 0.01$, $P > 0.05$, ns. Single data points and mean ± SEM of four biological replicates are shown). Source data are provided as a Source Data file.

Discussion

Present studies demonstrate that protein phosphatase PfPPM2 is a versatile enzyme as it regulates both asexual and sexual development of *P. falciparum*. While its *P. berghei* homologue is dispensable for asexual development, its disruption results in slow growth of this rodent parasite (https://plasmogem.umu.se/pbgem/)[8] and results in reduced gametocytemia as well as lower female:male gametocyte ratio as well as ookinete differentiation[5]. However, the mechanism via which PPM2 regulates parasite development had remained unclear. Conditional depletion of PfPPM2 revealed that it regulates the division of the *P. falciparum* and the phosphoproteomics studies revealed that PfPPM2 influences the phosphorylation of several proteins implicated in epigenetic regulation and translation (Supplementary Table 1), which included histone H3 and H3.3 and HP1. We went on to confirm

https://doi.org/10.1038/s41467-025-59476-w

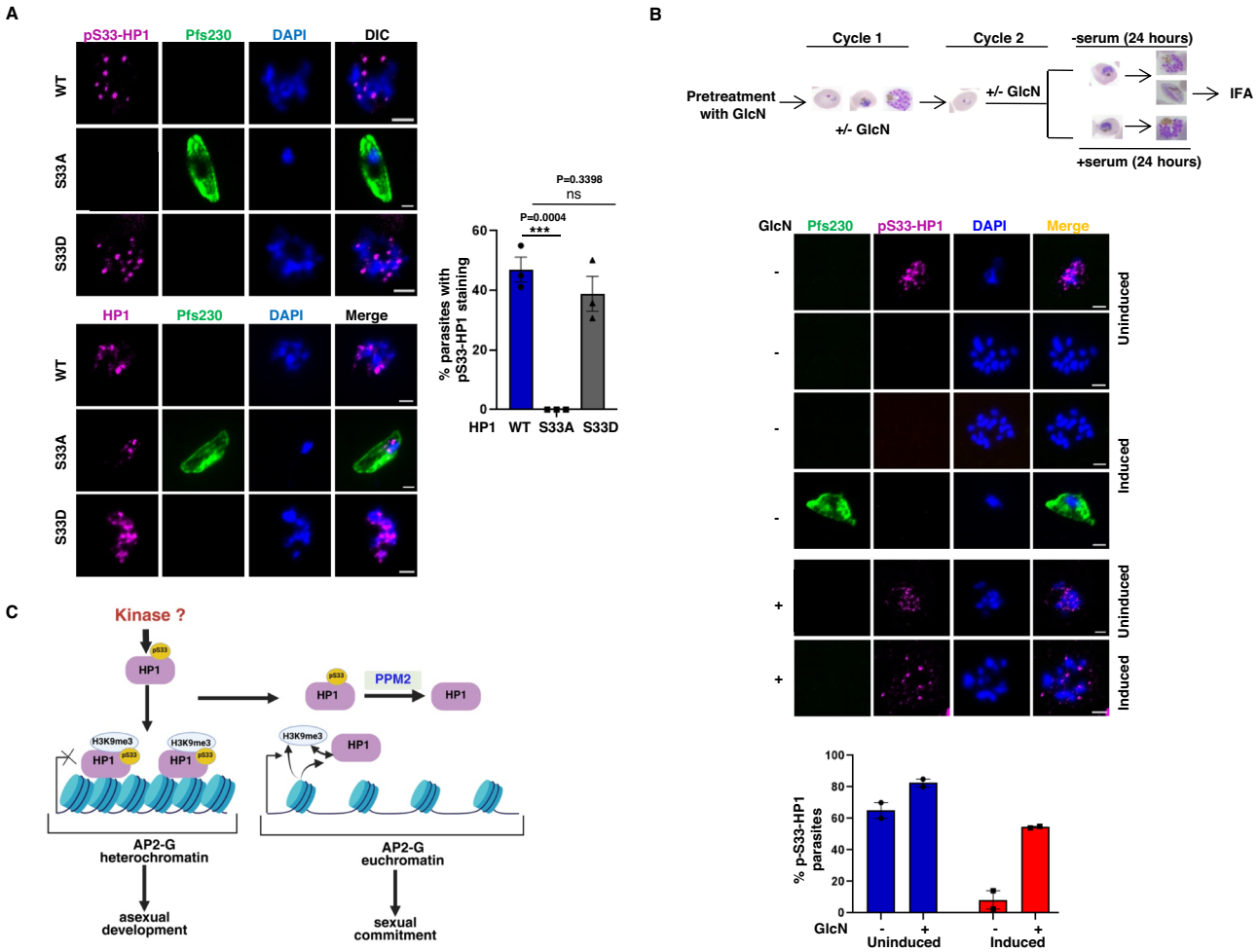

Fig. 6 | Dephosphorylation of HP1 is a novel signal for sexual differentiation of the parasite. A IFA was performed on thin blood smears of HP1/S33A/S33D-GFP-DD parasites cultured in the presence of Shld-1 using anti-pS33-HP1 and anti-Pfs230 antibodies, revealed that pS33-HP1 was present mainly in the asexual stages (HP1/HP1S33D) but it was absent from HP1-S33A parasites, majority of which were gametocytes (Statistical analysis was performed using One-way ANOVA, $^{***}P < 0.001$, $p > 0.05$ ns-non-significant, $n > 120$ parasites were counted in each condition. Single data points and mean ± SEM of three biological replicates are shown). Scale bar = 2 µm. **B** Sexual conversion of PfPPM2-HA-glmS^{NF54} cultured in the absence or presence of GlcN was induced by serum depletion as indicated in the schematic. IFA was performed on parasites pre- and post-induction using anti-pS33-HP1 and anti-Pfs230 antibodies. % pS33-HP1 positive parasites in each condition were determined ($n > 80$ parasites were counted in each condition. Single data points and mean ± SEM of two biological replicates are shown). Scale bar = 2 µm. **C** Schematic illustrates a novel signalling pathway in *P. falciparum*. Present studies demonstrate that PfPPM2 is important for both asexual division and sexual differentiation of *P. falciparum*. A yet to be identified kinase phosphorylates HP1 at S33, which is important for asexual development and division. S33-HP1 phosphorylation promotes its association with H3K9me3 and maintenance of heterochromatin state is critical for asexual division. PfPPM2 mediated dephosphorylation of HP1 at S33 prevents the interaction of HP1 with H3K9me3 and promotes euchromatin formation and derepression of AP2-G, which is critical for sexual differentiation. Created in BioRender. Sharma, P. (2025) https://BioRender.com/arwn5m3. Source data are provided as a Source Data file.

that the dephosphorylation of histone H3 at S10 and S28 and that of HP1 at S33 was prevented upon PfPPM2 depletion. The phosphorylation of histone H3 N-terminal tail at S10 and S28 in mammals and yeast has been associated with mitosis and transcriptional control, respectively[25,36]. Interestingly, H3 phosphorylation regulates distinct processes like stabilizing chromosome condensation during mitosis which contributes to transcriptional repression and activation during the interphase[37]. In addition, these sites need to be dephosphorylated by phosphatases like PP1 in mammalian cells failing which there is mitotic arrest[25,36]. While phosphorylation of these sites has been reported in *P. falciparum*[22], there is almost no information on their role in the parasite biology. It is possible that dephosphorylation of Histone H3 and possibly its variant H3.3 by PfPPM2 may also be critical for parasite division. Interestingly, transcriptome analysis revealed that several genes implicated in cell division like Centrin-1, Centrin-4, PCNA and genes involved in translation were deregulated upon PfPPM2 depletion, which was consistent with observed defects in PfPPM2-depleted parasites (Supplementary Fig. 9). The fact that HP1-overexpression prevented defects in asexual development and parasite division (Fig. 4A,B) also suggested that chromatin remodelling via phosphorylation of proteins like HP1 and histone H3 may contribute to parasite division. We observed defects in spindle biogenesis in PfPPM2-depleted parasites (Fig. 1F, Supplementary Fig. 3B,C). Since no major targets of PfPPM2 identified by phosphoproteomics relate to these processes, it is reasonable to suggest these are likely to be an outcome of arrested division.

Strikingly, H3K9me3 levels were significantly higher in PfPPM2-depleted parasites (Fig. 3F). In *P. falciparum*, H3K9me3-marked heterochromatin along with HP1 contributes to the repression of genes like AP2-G, which is involved in sexual commitment and selective expression of var gene family members that code for proteins exported to the host surface and are involved in evasion from the host immune system. AP2-G, which is involved in sexual commitment, is one of the few euchromatic genes which is silenced by HP1[27,33].

Consistent with higher H3K9me3 (Fig. 3F), the expression of AP2-G was reduced upon PfPPM2 depletion (Fig. 3D), which could be explained by enhanced occupancy of both H3K9me3 and HP1 on AP2-G locus (Fig. 3E). PfHP1-H3K9me3 interaction is critical for maintaining the H3K9me3 marks, which represses the expression of genes like AP2-G and prevents sexual differentiation. HP1 also regulates mutually exclusive expression of Var genes present at heterochromatic loci and in turn contributes to antigenic variation of PfEMP1[27]. Since present studies were focussed on asexual and sexual development of the parasite, regulation of var genes was not investigated, although transcriptome analysis suggested several var genes that normally exhibit mutually exclusive expression were aberrantly expressed upon PfPPM2 depletion (Supplementary Fig. 9). It is possible that deregulation of HP1 causes aberrant expression of var genes, which was hinted by the fact that the expression of VarB, one of the targets of HP1-H3K9me3[27], was reduced upon PfPPM2 depletion (Supplementary Fig. 9C).

The PfPPM2-target phosphorylation site S33 on HP1 is present in its chromodomain via which it interacts with H3K9me3[34,38]. It is clear from present studies that optimal phosphorylation state of S33-HP1 is critical for its function in asexual development and division as its hyperphosphorylation inhibits asexual development whereas hypophosphorylation causes sexual conversion of the parasites. In PfPPM2-depleted parasites, HP1-S33 is hyperphosphorylated (Fig. 3A, B) resulting in impaired asexual division and sexual conversion (Figs. 1D, 3C). The overexpression of HP1 could overcome these defects to some extent in PfPPM2-depleted parasites (Fig. 4A, Supplementary Fig. 6C). It is possible that the availability of more WT-HP1 molecules overcame the effects of its S33-hyperphosphorylated form in PfPPM2-depleted parasites and HP1 could undergo the cycles of phosphorylation and dephosphorylation, which seems to be relevant for its function in division and differentiation of the parasite. The phospho-deficient (S33A) and phospho-mimicking (S33D) mutants of HP1 recapitulated the hypo- and hyper-phosphorylated forms of HP1-S33, respectively. S33A promoted sexual conversion of the parasite whereas S33D caused arrest in asexual development. The fact that S33A mutant- which induces gametocyte formation or conversion- exhibited reduced interaction with H3K9me3 (Fig. 5E) fitted in well with previous findings which suggested that the loss of HP1 and H3K9me3 result in enhanced AP2-G expression and gametocyte formation[27,29,33]. It was also interesting to note that H3K9me3 levels were much lower in S33A mutant (Fig. 5E), which was consistent with higher H3K9me3 in PfPPM2-depleted parasites (Fig. 3F). Previous studies have indicated that upon binding H3K9me3, HP1 also recruits histone methyl transferases (HKMTs) to enhance H3K9me3 levels[39]. We could not perform IP from gametocytes due to some technical issues like the inability to obtain large number of gametocyte population. Nevertheless, these and other reported studies indicate a strong correlation between dephosphorylation of HP1 at S33, loss of interaction with H3K9me3 and sexual conversion of the parasite.

These data explained the reduced expression of AP2-G in PfPPM2-depleted parasites (Fig. 3D) that exhibited impaired sexual conversion (Fig. 3C), which was supported by the fact that S33A mutant overexpressing parasites- resembling PfPPM2 activated state-constitutively expressed AP2-G (Fig. 5D) and promoted sexual conversion (Fig. 5B,C). Consistent with this notion, pS33-HP1 was mainly detected in asexual parasites and was absent from gametocytes (Fig. 6A,B). Importantly, PfPPM2-depletion caused a significant increase in pS33-HP1 in asexual parasites (Fig. 6B) and corroborated well with reduced gametocytes formed by these parasites (Fig. 3C). Therefore, it is reasonable to suggest that dephosphorylation of HP1 is a signal which promotes sexual differentiation of malaria parasite by above-mentioned mechanism (Fig. 6C). It will be important to identify the kinase which phosphorylates HP1-S33 to promote asexual division and prevent sexual conversion. Since the phosphorylation of HP1 seems to regulate asexual replication of the parasite, one of the possibilities is that members of protein kinases implicated in cell division that are also present in *Plasmodium*[4], phosphorylate HP1. Given HP1 overexpression overcomes defects in parasite division as a result of PfPPM2-depletion (Fig. 4A and B), suggested that the regulation of HP1 may also be critical for parasite division. Previous studies indicate that HP1 depletion also results in parasite cell cycle arrest[27]. Interestingly, HP1-S33D mutant, which mimics hyperphosphorylated form of HP1 at S33, also exhibited severe growth arrest. Therefore, PfPPM2 seems to maintain the phosphorylation of S33 at optimal levels, which appears to be necessary for asexual development of the parasite- its hypophosphorylation results in sexual differentiation whereas hyperphosphorylation causes arrest in asexual development (Fig. 6C).

Present studies also indicate that PfPPM2 may promote mRNA translation or protein synthesis by preventing eIF2α phosphorylation by keeping eIF2α kinase PK4 in check (Supplementary Fig. 5). Alternatively, it may regulate dephosphorylation of eIF2α. Given that protein synthesis is important for cell cycle progression[16], it is possible that PfPPM2 may regulate parasite division by also regulating this process.

In summary, present studies demonstrate that PfPPM2 regulates both asexual division as well as conversion of parasites to sexual forms. It is evident that the regulation of HP1 dephosphorylation by PfPPM2 may be directly responsible for its ability to convert parasites to gametocytes. There are several possible direct or indirect interactions by which it may regulate parasite division. Its ability to regulate dephosphorylation of HP1 and chromatin remodelling proteins like histone H3 may be critical for parasite division, which was indicated by a reduced number of merozoites in PfPPM2-depleted parasites. These parasites exhibited defects in spindle formation, which may cause arrested division or may be an outcome of arrested division. The ability of PfPPM2 to regulate protein synthesis via PK4-eIF2α may also contribute to cell division as protein synthesis is critical for this process although direct evidence for the role of protein synthesis in division of malaria parasite is needed.

Methods

Parasite cultures

Plasmodium falciparum strains 3D7 and NF54 were obtained from *BEI* resources, Malaria Research and Reference Reagents Resource Centre (MR4), American Type Culture Collection (ATCC). Parasites were maintained in O^+ human erythrocytes (5% hematocrit) in RPMI-1640 supplemented with 0.5% AlbumaxII and 50 µg/mL hypoxanthine (cRPMI1640). Cultures were maintained at 37 °C under a mixture of 5% CO_2, 3% O_2, and 91.8% N_2 or 5% CO_2. Fresh erythrocytes were used to dilute parasites with fresh culture media to maintain 3–5% parasitemia at 5% haematocrit[40]. For culturing various transgenic lines, relevant drugs were used as described above. Parasite synchronization was carried out using sorbitol as described previously[41].

Generation of plasmid constructs and transfection of parasites

PfPPM2-3xHA-GlmS$^{3D7/NF54}$. In order to fuse *PfPPM2* with *glmS* and introduce a 3xHA tag at the C-terminus, a homology region corresponding to its 3'-end PfPPM2 was PCR amplified using primers (1/2) from *P. falciparum* 3D7 genomic DNA and cloned in pGlmS-SLI vector (a kind gift from Prof. Alan Cowman and further modified by Dr. Rahul Rawat by incorporating 2 A skip-NeoR cassette) using sites for *BglII* and *PstI*. Subsequently, PfPPM2-3xHA-glmS construct was then transfected in 3D7 and NF54 parasites. For the transfection of this and other plasmids described below, 8–10% ring stage parasites were electroporated with ~100 µg plasmid DNA. Parasites were maintained initially on 2-10 nM WR99210 followed by 400 µg/ml of G418 for selection linked integration. A mixed population of parasites, which included both integrants and wild type parasites, was observed upon genotyping of drug-selected parasites. The mixed population was subjected to

limited dilution cloning, the clones obtained after cloning were verified for correct 5′ and 3′ integration and the absence of the wild type unaltered region by genotyping PCR. PCR amplicons were sequenced for further confirmation. Genotyping was performed by using sets of PCR primers indicated in Supplementary Table 2.

PfPPM2-3xHA-GlmS$^{NF54:HP1/HP1-S33A-Flag}$. To generate pSLI-3x-Flag-yDHODH-BSD vector, first amplification of 2A-yDHODH fragment was done from pSLI-N-sandwich loxP vector[42] using primer (7/8) and cloned using *KpnI* and *XhoI* sites in pSLI-HA-glmS-BSD (a kind gift from Dr. Asif Mohmmed and further modified by Dr. Rahul Rawat by incorporating 2 A skip-NeoR cassette) vector to yield pSLI-3x-Flag-2A-yDHODH-BSD, which resulted in the replacement of the 3xHA-tag by 3xFlag coding sequence and introduction of 2 A skip peptide along with yDHODH cassette and removal of NeoR and glmS sequence. For tagging HP1 at the C-terminal end with 3x Flag tag, 3′- homology region was amplified from 3D7 genomic DNA using primer (9/10) and cloned using *SpeI* and *KpnI* sites to generate pSLI-HP1-3x-Flag-yDHODH-BSD construct. For generating, S33A-mutant tagged with flag, PCR primers (11/10)-in which codons for S33 were replaced with those for A-were used to clone the homology region using *SpeI* and *KpnI* sites of pSLI-3x-Flag-yDHODH-BSD vector. This construct was transfected in PPM2-HA-glmS^{NF54} parasite line and subsequently transgenic parasites were selected by using blasticidin (2.5 μg/ml) and recombinants were enriched using 1.5 μM DSM-1 and drug resistant parasites were genotyped for 5′-and 3′-integration and to check for the unmodified wild type locus of HP1. The desired mutation was confirmed by Sanger sequencing.

PfPPM2-HA-glmS$^{Nf54:}$HP1-GFP^{OE} or HP1/S33A/S33D-GFP-DD. HP1 was cloned in either pARL-GFP with BSD (a kind gift from Dr. Mohmmed Asif) or pARL-GFP-DD vector, which was modified as described below. For generating the pARL-HP1-GFP-DD, HP1 was amplified by PCR from 3D7 genomic DNA using primers (16/17) and GFP coding sequence was amplified from cpARL-GFP-BSD vector using primers (18/19) and the destabilization domain (DD) was amplified using primers (20/21) from pTEX-HA-DD vector. The HP1 and GFP domain was fused by overlapping PCR using primer (16/19) and GFP and DD domain was fused together using primer (18/21). The final overlapping PCR to obtain HP1-GFP-DD fused together was done by using primer set (16/21) and cloning was performed using *KpnI* and *AvrII* restriction sites of cpARL-GFP-BSD vector. S33A mutations in HP1 were generated by site directed mutagenesis using primers (22/23) and S33D mutation was generated using primers (24/25), which were confirmed by sequencing. Subsequently, mutants were cloned in pARL-GFP-DD vector like the WT HP1. For pARL-HP1-GFP construct, HP1 was cloned in pARL-GFP-BSD vector using primers 16/17′ using *KpnI* and *AvrII* sites.

These plasmid constructs were transfected in PPM2-HA-glmS^{NF54} for generating PfPPM2-HA-glmS$^{Nf54:}$HP1-GFP^{OE} or NF54 parasites for HP1/S33A/S33D-GFP-DD parasites and were selected with 2.5 μg/ml of Blasticidin.

Growth rate assays

PfPPM2-HA-glmS parasites were cultured in the presence of 10 nM WR99210 and 400 μg/ml G418 and PfPPM2-HA-glmS$^{Nf54:}$HP1-GFP^{OE} parasites were cultured in the presence of 10 nM WR99210 (Jacobus Pharmaceuticals), 400 μg/ml G418 (TM Media; 3341) and 2.5 μg/ml of Blasticidin (Sigma-Aldrich;15205). Subsequently, ring stage parasites were seeded at ~0.5% parasitemia at 2% hematocrit after synchronisation. For the depletion of PfPPM2, ring stage parasites were typically treated with 2.5 mM glucosamine (GlcN) (Sigma-Aldrich; G1514) for one cycle and parasite growth was assessed at an interval of 24-h for additional 144-h. For growth rate assays with HP1/S33A/S33D-GFP-DD lines, parasites were synchronized and seeded at ~0.5% ring parasitemia and parasites were cultured in the presence or absence of Shield-1 (250 nM) (Cheminpharma, LLC, USA) for two cycles. Typically, samples were collected after every 24 h for making thin blood smears as well as FACS analysis.

Giemsa-stained thin blood smears were microscopically examined and various parasite stages (rings, trophozoite, schizonts) were counted to determine the parasitemia. For determining parasitemia using flow cytometry, samples were fixed with 1% PFA and 0.0075% glutaraldehyde solution and kept on an end-to-end rocker for 15 min. After completion, samples were either stored at 4°C or processed directly for Hoechst 33342 staining for 10-min at 37°C. Samples were then washed at least twice with FACS buffer followed by analysis on BDverse (BD biosciences) for 10,000–100,000 events per sample[43]. The data was processed and analyzed using FlowJo V.10.10.0 software.

Assessment of parasite division

Parasite lines were synchronized and GlcN treatment was provided for one cycle, E64 (10 μM) (Sigma-Aldrich; E3132) was added at ~40 h.p.i. (cycle 1) schizonts for 4–5 hours. Thin blood smears were prepared, stained with Giemsa images of mature schizonts were captured on a Leica bright field microscope. The numbers of merozoites from at least 50 schizonts for each condition, per replicate, were counted and average number of merozoites per schizont was determined.

Gametocyte conversion assay

For inducing gametocytogenesis, sexual conversion was induced as previously described with some minor modifications[31,44]. Briefly, PPM2-HA-glmS^{NF54} parasites were treated with 2.5 mM GlcN for one cycle (pre-treatment). Subsequently, parasites were seeded at 2% rings in 5% haematocrit. In the next cycle, when parasitemia reached ~10%, gametocytogenesis was induced by replacing serum containing complete RPMI-1640 (cRPMI) medium with serum free medium containing Fatty acid free BSA (Sigma Aldrich; A6003), Oleic acid (Sigma Aldrich; O1008), Palmitic acid (Sigma Aldrich; P0500). After ~24-h, serum free medium was removed followed by supplementation of cRPMI and treatment with 50mM N-acetyl-D-Glucosamine (Sigma-Aldrich; A8625) was provided for 5 days to eliminate the asexual parasites unless indicated otherwise. Giemsa smears were made periodically and the number of gametocytes was counted at day 5 p.g.i. Sexual conversion rates were determined by counting gametocytes formed at day 5 relative to the initial parasites, which were mainly asexual rings[45,46]. In order to assess the sexual conversion of the HP1/S33A/S33D-GFP-DD parasites, sorbitol synchronization was performed at the ring stage and parasites were left untreated or treated with Shld-1 (250 nM). Subsequently, IFAs were performed after 4–6 days on blood smears using anti-GFP (Roche; SKU-11814460001) and anti-Pfs16 (MRA-1276) or anti-Pfs230 (MRA-878A) antibodies. The number of Pfs16/Pfs230-stained parasites that represented gametocytes was counted. Since pS33-HP1 antibody (Antagene) was raised in rabbits, co-staining was done using anti-Pfs230 which was raised in mice.

Parasite invasion assay

Invasion assays were carried out as described previously with slight modifications[43,47]. Following sorbitol treatment, parasites were cultured in the presence or absence of glucosamine (2.5 mM GlcN) for one cycle. After 90-h (cycle 1, schizonts), MACS columns (Miltenyi Biotec) were used to purify schizonts, which were washed twice and resuspended in RPMI 1640 medium with fresh RBCs to achieve 2% hematocrit. Invasion experiments were performed using 0.5–1% schizont / 2% hematocrit in a 6-well plate in a gas chamber equilibrated with gas mixture described above at 37°C along with shaking at 80 rpm and samples were collected every 2-h. Flow cytometry was used to determine the number of schizonts and rings for which parasites were fixed using 1% PFA + 0.0075% glutaraldehyde in FACS solution (0.3% BSA + 0.02% Sodium azide in 1xPBS solution) followed by staining with

Hoechst 33342 (1:10,000 dilution) which was prepared in FACS solution. Flow cytometry data was acquired using BD FACS verse and analysed using FlowJo V.10.10.0 software (Tree Star, Ashland, OR).

Immunofluorescence Assay (IFAs)

Immunofluorescence assays (IFA) were performed on thin blood smears as previously described[48]. Briefly, air-dried thin blood smears were fixed with cold methanol and acetone mix (1:1, v:v) for 2-min followed by blocking with 3% BSA for 45-min at room temperature. Subsequently, smears were incubated with primary antibodies for 12-h at 4 °C. After washing with blocking buffer, Alexa fluor mouse/rabbit 488/594-labelled secondary antibodies were added (Invitrogen) for 2-h at ambient temperature. Finally, Vecta shield mounting media was used (Vector Laboratories Inc.), which contained DAPI to label nuclei. Fluorescence microscopy was performed using Axio Imager Z1 microscope or a LSM980 confocal microscope (Carl Zeiss). The images were processed using AxioVision 4.8.2 or Zeiss ZEN blue 3.1 or 3.9 software and best representative z-stacks were used for illustrations in the figures unless indicated otherwise.

Ultrastructure-Expansion Microscopy

PfPPM2-HA-glmS^{Nf54} parasite lines were synchronized and GlcN treatment was provided for one cycle. Further, at ~92–94 h.p.i. (cycle 1) schizonts were fixed using 4% para-formaldehyde (PFA) in PBS at 37°C for 20-min. Sample preparation of *P. falciparum* parasites for U-ExM was performed as previously described with slight modifications[12,49]. Immuno-labelling was performed using primary antibodies against α-tubulin (1:500 dilution, SAB3501072, Sigma) anti-centrin antibody (1:200 dilution, Sigma 20H5), anti-HA antibody (1:200 dilution, 12CA5 Roche), anti-PfGAP45 antibody (1:500 dilution, generated previously by Sharma laboratory) and sytox (S11830, Invitrogen). Secondary antibodies anti-mouse Alexa 568 (A21134, Invitrogen), anti-rabbit Alexa 488 (A27034, Invitrogen) and were used at dilutions 1:1000. Images were acquired using a LSM980 confocal microscope (Carl Zeiss) and images were processed using Zeiss ZEN blue 3.1 or 3-.9 software. Maximum Intensity Projection (MIP) was provided for all U-ExM images. The laser power was maintained constant for imaging control and treated samples unless indicated otherwise.

Immunoblotting

Parasite cultures were collected and iRBCs were lysed using 0.05% saponin (w/v) followed by incubation on ice for 10-min. Centrifugation at 8000 rpm was done to isolate the parasite pellet, which was washed three times with pre-chilled PBS. The parasite pellet was re-suspended in lysis buffer (10 mM Tris pH 7.5, 100 mM NaCl, 5 mM EDTA, 1% Triton X-100, and complete protease inhibitor cocktail; Roche Applied Science) or 2% SDS and then homogenized by either passing the solution through a 26-gauge needle or by using sonication at 60% amplitude for 20-sec (1-sec ON/OFF). The supernatant from the centrifugation of the lysates at 14,000 g for 30-min at 4 °C was used to estimate the amount of protein using a BCA protein estimation kit (Pierce). Nuclear protein lysates were prepared as described below.

After SDS-PAGE, proteins were transferred to nitrocellulose membrane and membranes with transferred proteins were blocked with 3% BSA/0.2% Tween 20 in 1xTBS (v/v) for 1-h. Primary antibody solutions were made in 3% BSA, diluted to the required concentration and membranes were incubated for 12-h at 4 °C. The membrane was then rinsed three times with 1xTBS/0.1% Tween 20 (TBS-T) and incubated with Horseradish Peroxidase (HRP) conjugated secondary antibody prepared in 3% skimmed milk/1xTBS-T or 3%BSA/1x TBS-T (used for phospho antibody-blots) for 2-h. The nitrocellulose membrane was once again washed with 1xTBS-T and detection was performed using West Pico or Femto chemiluminescence substrate from Pierce (USA) after exposure of the membrane to X-ray films.

Immunoprecipitation

Immunoprecipitation was performed on nuclear lysates. For making the nuclear lysate, fractionation was performed as previously described[28,29] with some minor modifications. Saponin-lysed infected red blood cells were lysed in ice-cold cell lysis buffer (20 mM HEPES pH 7.9, 10 mM KCl, 1 mM EDTA, 1 mM EGTA, 1 mM DTT, protease inhibitors) for 5-min. After a 5-min centrifugation at 5200 rpm (2500xg), the cytosolic extract was collected and stored at -80°C and the nuclei obtained were treated with DNase I and RNase A [(20 mM Hepes pH 7.4, 10 mM NaCl, 5 mM MgCl2, 1 mM CaCl2, 0.1% NP-40, 1x protease inhibitor (Roche Diagnostics), 1x PhosSTOP (Roche Diagnostics), 0.5U/μl DNase I, 1 μg RNase A] and incubated in 250 μl reaction volume for 5-min at 37°C). Reactions were adjusted to 500 μl using 2x high salt extraction buffer (20 mM Hepes pH 7.4, 1 M NaCl, 6 mM EDTA, 2 mM EGTA, 2 mM TCEP, 1x protease inhibitor (Roche Diagnostics), 1x PhosSTOP (Roche Diagnostics), 50% Glycerol, 0.1%NP-40) and nuclear proteins were extracted in 2.5 pellet volume of high salt extraction buffer (20 mM Hepes pH 7.4, 500 mM NaCl, 3 mM EDTA, 1 mM EGTA, 1 mM TCEP, 1x protease inhibitor (Roche Diagnostics), 1x PhosSTOP (Roche Diagnostics), 25% Glycerol, 0.1%NP-40) by vortexing for 30-min at 4 °C. After centrifugation at 20,800 g at 4°C for 30-min, supernatant was separated immediately and used for IP experiments after dilution. High salt nuclear extracts were diluted to 250 mM NaCl using dilution buffer (20 mM Hepes pH 7.4, 1 mM EDTA, 1 mM TCEP, 1x protease inhibitor (Roche Diagnostics), 1x PhosSTOP (Roche Diagnostics), 25% Glycerol).

For immunoprecipitation, ~200 μg of nuclear protein lysate was typically used and incubated with relevant antibodies at 4°C for 12-h followed by incubation with protein A + G sepharose beads for 5-h. After 3x washes with wash buffer, beads were boiled at 95 °C for 10-min. After boiling, supernatant was used for immunoblotting along with the input. After electrophoresis SDS-PAGE, lysate proteins were transferred to a nitrocellulose membrane and immunoblotting was performed as described previously[50,51] using specific antibodies and blots were developed using SuperSignal® West Pico or Femto chemiluminescence Substrate (Thermo Scientific) by following manufacturer's instructions.

Generation of pS33-HP1 antibody and anti-HP1 antisera

Custom antibodies were raised against HP1 phosphorylated at S33 (anti-pS33-PfHP1) or an unphosphorylated version of the S33 (HP1 non-phospho) by M/s Antagene Inc. For phospho antibody generation, a peptide with a sequence: Cys-YLVKWKGY(p)SDDENTW and for non-phospho peptide Cys-YLVKWKGYSDDENTW was used for immunization. Phospho-antibodies were purified by affinity chromatography using these peptides and validation was done by the manufacturer by performing ELISA. For Western blotting, 1:100-200 dilution of the purified phospho and non-phospho antibody was used and for IFAs 1:25 of anti-pS33HP1 was used. Total HP1 antisera were raised in rabbit against bacterially expressed HP1 was a gift from Dr. Krishanpal Karmodiya, IISER Pune or was also raised against the same recombinant protein by immunizing rabbits. The approval from Institute Animal Ethics Committee of NII was taken for this purpose and recommended protocol and ethical regulations were followed.

SUrfaceSEnsing of Translation (SUnSET) assay or Puromycin incorporation assay

Protein synthesis was assessed using a SUnSET assay[21,52] for which parasites were treated with 1 μM puromycin (structural analog of tyrosyl-tRNA) (Sigma Aldrich; P8833) for 1-h. Parasites were harvested at trophozoite and schizont stages and protein lysates were prepared using 2% SDS, which were subjected to Western blot analysis. To

ensure equal loading of proteins, the nitrocellulose membrane was stained with Ponceau S before blocking with 3% BSA for 1-h. After blocking, blots were incubated with anti-puromycin antibody (Merck; MABE343) overnight at 4°C. Subsequently, blots were washed with 1xTBST and incubated with α-FCY-subclass 2a mouse IgG antibody for 1-h. The blots were developed by Pico or Femto chemiluminescence substrate from Pierce (USA) after exposure of the membrane to X-ray films.

Quantitative RT-PCR

RNA isolation was carried out using TRIzol reagent (G Biosciences). Real time PCR was carried out using CFX96 Real Time PCR detection system (Biorad). Quantification of the expression was done by determining SYBR green incorporation in the amplicons (G Biosciences). For qRT-PCR, 1 µg of DNase free RNA was used for cDNA synthesis using Verso cDNA synthesis kit (Thermo scientific), as per the manufacturer's recommendation. Random hexamers supplied with the kit were used for the cDNA synthesis. 18srRNA or Actin were used as a housekeeping gene for normalization. A typical PCR reaction conditions were: 95 °C for 3-min, 95 °C for 15-sec, 60 °C for 1-min and 40 cycles. Finally, the relative fold change in gene expression was determined as $2^{-\Delta\Delta Ct}$. Primers details for the qRT-PCR are given in (Supplementary Table 2).

RNA sequencing

Nf54 (control) and PfPPM2-HA-glmS^{Nf54} lines were treated with GlcN and were harvested at first cycle at the schizont stage (42-44 h.p.i) in triplicate. RNA isolation was performed using the phenol-chloroform extraction method, followed by quantification using a Qubit fluorometer (Thermo Fisher Scientific). For all samples, 1 µg of RNA was used as an input for mRNA enrichment using the NEBNext Poly (A) mRNA magnetic isolation module (New England Biolabs #E7490S) according to the manufacturer's instructions. A NEBNext Ultra II RNA library prep kit for Illumina (New England Biolabs #E7770S) was used to prepare the library according to the manufacturer's instructions, and quality checks were performed using Agilent TapeStation. Paired-end sequencing was performed on an Illumina Nextseq550 platform (75 bp read length).

RNAseq Data Analysis

RNA-seq data analysis was performed as described below. The quality of sequenced samples was accessed using FASTQC and adapters were trimmed with Trim Galore (https://doi.org/10.5281/zenodo.5127899) and cutadapt (https://doi.org/10.14806/ej.17.1.200). High quality trimmed reads were aligned in paired-end mode to *Plasmodium falciparum* 3D7 genome ver. 66 using HISAT2[53] with default settings. Differential gene expression analysis was performed using DEseq2[54] using standard analysis protocol. Gene set enrichment analysis was performed using ClusterProfiler[26] and results were plotted with custom R and python scripts.

Chromatin Immunoprecipitation (ChIP) and ChIP-qPCR

Parasites cultured in the presence (2.5 mM GlcN) or absence of glucosamine (GlcN) and were harvested at the end of first cycle at ~90 h.p.i by fixing the cells. The iRBCs were cross linked using 1% formaldehyde (Thermo Scientific, 28908) for 10-min. Subsequently, 150 mM glycine was then added for quenching the cross-linking reaction for 10-min at ambient temperature followed by centrifugation at 6000 rpm at 4 °C for 5-min. Pellet was washed three times using 1xcold PBS (supplemented with protease inhibitors) before proceeding for lysis. Sample homogenization was performed using swelling buffer (25 mM Tris pH 7.9, 1.5 mM MgCl2, 10 mM KCl, 0.1% NP 40, 1 mM DTT, 0.5 mM PMSF, 1 × PIC) followed by cell lysis in sonication buffer (10 mM Tris–HCl pH 7.5, 200 mM NaCl, 1% SDS, 4% NP-40,1 mM PMSF, 1X protease inhibitor cocktail). First, pre-clearing was performed for 2-h at 4 °C by incubating the chromatin fraction with- protein A conjugated sepharose beads (G-Biosciences) with continuous gentle mixing. Pre-cleared lysate was incubated with the relevant antibody for 12-h at 4 °C followed by incubation with saturated Protein A Sepharose beads for 4-h at 4 °C. Bound chromatin was finally washed with low salt wash buffer, high salt wash buffer, LiCl wash buffer, TE wash buffer and eluted using ChIP elution buffer (1% SDS, 0.1 M sodium bicarbonate). Both IP sample and input were reverse cross-linked using 0.3 M NaCl overnight at 65 °C along with RNase followed by Proteinase K treatment at 42 °C for 1-h. Finally, bound DNA was purified using phenol-chloroform precipitation. The occupancy of genes of interest was assessed by ChIP-qPCR using the SYBR Green Master Mix (G Biosciences). The amount of template used for qPCR was 1 µl of 1% input DNA and 2 µl of undiluted ChIP DNA. qPCR was performed using previously described primers corresponding to AP2-G and Pfs16 locus (Supplementary Table 2)[27]. The amount of DNA amplified was compared to the input and % recovery of bound DNA was determined.

Phosphoproteomics and Mass spectrometry

Proteomics Studies

Cell lysis and protein extraction and TMT labeling. The 3D7 or PfPPM2-HA-glmS^{3D7} parasites were cultured and synchronized using sorbitol. Ring stage parasites were treated with glucosamine for 72-h. The parasites were subsequently harvested upon maturation to schizonts in cycle 1 (~ 44 hours post-infection), by lysing the infected red blood cells with saponin. The parasite pellet was washed and dissolved in protein extraction buffer (50 mM triethylammonium bicarbonate (TEAB, Sigma Aldrich; T7408), 2% SDS, and 1X protease and phosphatase inhibitors) followed by sonication and centrifugation. Protein estimation was done by Bicinchoninic Acid assay (BCA estimation kit, Sigma Aldrich; 23225). Equal amounts of protein were taken from all sets of parasites and subjected to reduction with 20 mM Dithiothreitol (DTT, Sigma Aldrich; D9779) at 60 °C for 30-min, followed by alkylation with 20 mM Iodoacetamide (IAA, Sigma Aldrich; I1149) for 10-min in the dark at ambient temperature. Subsequently, proteins were digested using trypsin and Lys-C mix (Promega, Madison, USA; V5073) used at a ratio of 100:1. Tryptic peptides were cleaned using a C18 column and dried with a SpeedVac concentrator (Thermo Fisher Scientific, USA). The peptides were quantified using the Pierce Quantitative Colorimetric Peptide Assay Kit (Sigma Aldrich; 23275). Further, 500 µg of peptides from each sample were processed for TMT labelling following manufacturer's instructions (Thermo Scientific; 90110). Labelling efficiency of >95% was achieved and the reaction was stopped by adding 8 µl of hydroxylamine. The labelled peptides were pooled, dried, and cleaned using C18 Sep-Pak cartridges (Waters, Milford, MA, USA; WAT054955).

Phosphopeptide enrichment and fractionation. 50 µg of the peptide sample was used for total proteome analysis, and the remaining sample was subjected to phosphopeptide enrichment. For the initial phosphopeptide enrichment, the TiO2 Phosphopeptide Enrichment Kit was utilized (Thermo Scientific; A32993). The subsequent enrichment step was performed on the collected flow-through using the High-Select Fe-NTA Phosphopeptide Enrichment Kit (Thermo Scientific; A32992). The eluents from both enrichment steps were combined and subjected to fractionation using C18 Stage Tips. A total of 24 fractions were collected and then concatenated into six fractions. The peptide samples were dried and dissolved in 0.1% formic acid (Thermo Scientific; 94318) prior to mass spectrometry analysis.

LC-MS/MS analysis by Data-Dependent Acquisition. Mass spectrometry analysis was performed on an Orbitrap Fusion Tribrid Mass Spectrometer linked to an Easy-nLC 1200 nano-flow UPLC system (Thermo Fisher Scientific, Germany). The peptide fractions were loaded on nanoViper column (2 cm, 3 µm C18 Aq) (Thermo Fisher

Scientific) and were then resolved on an analytical column (75 μm × 15 cm, C18, 2 μm particle size) (Thermo Fisher Scientific). The peptides were separated by passing solvent A (0.1% formic acid) and solvent B (80% acetonitrile in 0.1% formic acid) using a gradient mode over a 120-min at a flow rate of 300 nl/min.

Data-dependent acquisition (DDA) mode was used for data acquisition. Precursor ions were acquired in full MS scan mode in the range of 400-1600 m/z, using an Orbitrap mass analyzer resolution of 120,000 at 200 m/z. An automatic gain control (AGC) target value of 2e5 with an injection time of 55 ms and dynamic exclusion of 30 seconds was used. The selection of the most intense precursor ions was performed at top speed DDA mode, selected using a quadrupole with an isolation window of 2 m/z. The filtered precursor ions were subsequently fragmented using higher-energy collision-induced dissociation (HCD) with 32 ± 3% normalized collision energy and MS/MS scans in the range of 110-2000 m/z were acquired by using Orbitrap mass analyzer with 30,000 mass resolution at 200 m/z. AGC target was set to 1e5 with an injection time of 200 ms. For each fraction, MS/MS data was acquired in duplicates.

Data analysis. MS/MS raw data was used to search against a combined protein database of *P. falciparum* 3D7 (downloaded from PlasmoDB web resource, version 46) and *Homo sapiens (RefSeq v92)* using SEQUEST and Mascot (version 2.4.1) via Proteome Discoverer v2.2 (Thermo Fisher Scientific) as described previously[47]. A fold change cut-off of 1.5 with a p value ≤ 0.05 was used to identify significantly altered phosphorylated proteins The phosphorylation fold changes were normalized with respect to the total proteome data as reported earlier[47,55]. Phosphosites that were identified differentially phosphorylated in two or more biological replicates were considered for the further analysis. The ptmRS node was used during the search to determine the probability of phosphorylation site localization and a ptmRS score ≥99% was used as a cut off. These proteins were then analyzed for the enrichment of biological processes using Gene Ontology (GO) analysis through PlasmoDB.

Densitometry and statistical analysis

Image J (NIH) software v1.54 was used to perform densitometry of Western blots. The band intensity of the loading control was used for normalization. Statistical analysis was performed using Graph Pad Prism v5 or 9 (Graph Pad software Inc USA). Data is represented as mean ± Standard error of mean (SEM), unless indicated otherwise and $p < 0.05$ was considered as statistically significant. No data was excluded from the analysis.

Reporting summary

Further information on research design is available in the Nature Portfolio Reporting Summary linked to this article.

Data availability

RNA sequencing data are submitted to Gene Expression Omnibus (GEO) under the accession number: GSE275086 and can be accessed using the following link. https://www.ncbi.nlm.nih.gov/geo/query/acc.cgi?acc=GSE275086. The mass spectrometry-based proteomics data have been deposited to the ProteomeXchange Consortium (http://proteomecentral.proteomexchange.org) via the PRIDE partner repository with the Dataset identifier PXD055390 and can be accessed using the following link https://www.ebi.ac.uk/pride/archive/projects/PXD055390. Source data are provided as Source Data file. Source data are provided with this paper.

References

1. World Malaria Report. Geneva: World Health Organization; 2022. Licence: CC BY-NC-SA 3.0 IGO. (2022).
2. Cowman, A. F., Healer, J., Marapana, D. & Marsh, K. Malaria: Biology and Disease. *Cell* **167**, 610–624 (2016).
3. Guttery, D. S., Zeeshan, M., Ferguson, D. J. P., Holder, A. A. & Tewari, R. Division and Transmission: Malaria Parasite Development in the Mosquito. *Annu Rev. Microbiol* **76**, 113–134 (2022).
4. Adderley, J. & Doerig, C. Comparative analysis of the kinomes of Plasmodium falciparum, Plasmodium vivax and their host Homo sapiens. *BMC Genom* **23**, 237 (2022).
5. Guttery, D. S. et al. Genome-wide functional analysis of Plasmodium protein phosphatases reveals key regulators of parasite development and differentiation. *Cell Host Microbe* **16**, 128–140 (2014).
6. Zhang, M. et al. Uncovering the essential genes of the human malaria parasite Plasmodium falciparum by saturation mutagenesis. *Science*, https://doi.org/10.1126/science.aap7847 (2018).
7. Mamoun, C. B. & Goldberg, D. E. Plasmodium protein phosphatase 2C dephosphorylates translation elongation factor 1beta and inhibits its PKC-mediated nucleotide exchange activity in vitro. **39**, 973 (2001).
8. Gomes, A. R. et al. A genome-scale vector resource enables high-throughput reverse genetic screening in a malaria parasite. *Cell Host Microbe* **17**, 404–413 (2015).
9. Wilkes, J. M. & Doerig, C. The protein-phosphatome of the human malaria parasite. *Plasmodium falciparum* **9**, 412 (2008).
10. Mamoun, C. B., Sullivan, D. J. Jr., Banerjee, R. & Goldberg, D. E. Identification and characterization of an unusual double serine/threonine protein phosphatase 2C in the malaria parasite Plasmodium falciparum. *J. Biol. Chem.* **273**, 11241–11247 (1998).
11. Prommana, P. et al. Inducible knockdown of Plasmodium gene expression using the glmS ribozyme. *PLoS One* **8**, e73783 (2013).
12. Liffner, B. et al. Atlas of Plasmodium falciparum intraerythrocytic development using expansion microscopy. *bioRxiv*, https://doi.org/10.1101/2023.03.22.533773 (2023).
13. Kono, M. et al. Evolution and architecture of the inner membrane complex in asexual and sexual stages of the malaria parasite. *Mol. Biol. Evol.* **29**, 2113–2132 (2012).
14. Liu, Y. et al. An inner membrane complex protein IMC1g in Plasmodium berghei is involved in asexual stage schizogony and parasite transmission. *mBio*, e0265224 (2024).
15. Cepeda Diaz, A. K., Rudlaff, R. M., Farringer, M. & Dvorin, J. D. Essential function of alveolin PfIMC1g in the Plasmodium falciparum asexual blood stage. *mBio* **14**, e0150723 (2023).
16. Polymenis, M. & Aramayo, R. Translate to divide: control of the cell cycle by protein synthesis. *Microb. Cell* **2**, 94–104 (2015).
17. Beck, J. R. et al. A novel family of Toxoplasma IMC proteins displays a hierarchical organization and functions in coordinating parasite division. *PLoS Pathog.* **6**, e1001094 (2010).
18. Zhang, M. et al. Inhibiting the Plasmodium eIF2alpha Kinase PK4 Prevents Artemisinin-Induced Latency. *Cell Host Microbe* **22**, 766–776 e764 (2017).
19. Zhang, M. et al. PK4, a eukaryotic initiation factor 2alpha(eIF2alpha) kinase, is essential for the development of the erythrocytic cycle of Plasmodium. *Proc. Natl Acad. Sci. USA* **109**, 3956–3961 (2012).
20. Thommen, B. T. et al. Genetic validation of PfFKBP35 as an antimalarial drug target. *Elife*. https://doi.org/10.7554/eLife.86975 (2023).
21. McLean, K. J. & Jacobs-Lorena, M. Plasmodium falciparum Maf1 Confers Survival upon Amino Acid Starvation. *mBio*. https://doi.org/10.1128/mBio.02317-16 (2017).
22. Dastidar, E. G. et al. Comprehensive histone phosphorylation analysis and identification of Pf14-3-3 protein as a histone H3 phosphorylation reader in malaria parasites. *PLoS One* **8**, e53179 (2013).

23. Komar, D. & Juszczynski, P. Rebelled epigenome: histone H3S10 phosphorylation and H3S10 kinases in cancer biology and therapy. *Clin. Epigenet.* **12**, 147 (2020).
24. Sawicka, A. & Seiser, C. Histone H3 phosphorylation - a versatile chromatin modification for different occasions. *Biochimie* **94**, 2193–2201 (2012).
25. Gil, R. S. & Vagnarelli, P. Protein phosphatases in chromatin structure and function. *Biochim Biophys. Acta Mol. Cell Res* **1866**, 90–101 (2019).
26. Yu, G., Wang, L. G., Han, Y. & He, Q. Y. clusterProfiler: an R package for comparing biological themes among gene clusters. *Omics: a J. Integr. Biol.* **16**, 284–287 (2012).
27. Brancucci, N. M. B. et al. Heterochromatin protein 1 secures survival and transmission of malaria parasites. *Cell Host Microbe* **16**, 165–176 (2014).
28. Flueck, C. et al. Plasmodium falciparum heterochromatin protein 1 marks genomic loci linked to phenotypic variation of exported virulence factors. *PLoS Pathog.* **5**, e1000569 (2009).
29. Filarsky, M. et al. GDV1 induces sexual commitment of malaria parasites by antagonizing HP1-dependent gene silencing. *Science* **359**, 1259–1263 (2018).
30. Perez-Toledo, K. et al. Plasmodium falciparum heterochromatin protein 1 binds to tri-methylated histone 3 lysine 9 and is linked to mutually exclusive expression of var genes. *Nucleic Acids Res* **37**, 2596–2606 (2009).
31. Flammersfeld, A. et al. A patatin-like phospholipase functions during gametocyte induction in the malaria parasite Plasmodium falciparum. *Cell Microbiol* **22**, e13146 (2020).
32. Josling, G. A. et al. Dissecting the role of PfAP2-G in malaria gametocytogenesis. *Nat. Commun.* **11**, 1503 (2020).
33. Kafsack, B. F. et al. A transcriptional switch underlies commitment to sexual development in malaria parasites. *Nature* **507**, 248–252 (2014).
34. Bannister, A. J. et al. Selective recognition of methylated lysine 9 on histone H3 by the HP1 chromo domain. *Nature* **410**, 120–124 (2001).
35. Armstrong, C. M. & Goldberg, D. E. An FKBP destabilization domain modulates protein levels in Plasmodium falciparum. *Nat. Methods* **4**, 1007–1009 (2007).
36. Qian, J., Lesage, B., Beullens, M., Van Eynde, A. & Bollen, M. PP1/Repo-man dephosphorylates mitotic histone H3 at T3 and regulates chromosomal aurora B targeting. *Curr. Biol.: CB* **21**, 766–773 (2011).
37. Perez-Cadahia, B., Drobic, B. & Davie, J. R. H3 phosphorylation: dual role in mitosis and interphase. *Biochem Cell Biol.* **87**, 695–709 (2009).
38. Bui, H. T. N., Passecker, A., Brancucci, N. M. B. & Voss, T. S. Investigation of Heterochromatin Protein 1 Function in the Malaria Parasite Plasmodium falciparum Using a Conditional Domain Deletion and Swapping Approach. *mSphere* https://doi.org/10.1128/mSphere.01220-20 (2021).
39. Loyola, A. et al. The HP1alpha-CAF1-SetDB1-containing complex provides H3K9me1 for Suv39-mediated K9me3 in pericentric heterochromatin. *EMBO Rep.* **10**, 769–775 (2009).
40. Trager, W. & Jensen, J. B. Cultivation of erythrocytic stages. *Bull. World Health Organ* **55**, 363–365 (1977).
41. Lambros, C. & Vanderberg, J. P. Synchronization of Plasmodium falciparum erythrocytic stages in culture. *J. Parasitol.* **65**, 418–420 (1979).
42. Birnbaum, J. et al. A genetic system to study Plasmodium falciparum protein function. *Nat. Methods* **14**, 450–456 (2017).
43. Theron, M., Hesketh, R. L., Subramanian, S. & Rayner, J. C. An adaptable two-color flow cytometric assay to quantitate the invasion of erythrocytes by Plasmodium falciparum parasites. *Cytom. A* **77**, 1067–1074 (2010).
44. Brancucci, N. M. B. et al. Lysophosphatidylcholine Regulates Sexual Stage Differentiation in the Human Malaria Parasite Plasmodium falciparum. *Cell* **171**, 1532–1544.e1515 (2017).
45. Llora-Batlle, O. et al. Conditional expression of PfAP2-G for controlled massive sexual conversion in Plasmodium falciparum. *Sci. Adv.* **6**, eaaz5057 (2020).
46. Coleman, B. I. et al. A Plasmodium falciparum histone deacetylase regulates antigenic variation and gametocyte conversion. *Cell Host Microbe* **16**, 177–186 (2014).
47. Rawat, R. S. et al. Protein kinase PfPK2 mediated signalling is critical for host erythrocyte invasion by malaria parasite. *PLoS Pathog.* **19**, e1011770 (2023).
48. Tonkin, C. J. et al. Localization of organellar proteins in Plasmodium falciparum using a novel set of transfection vectors and a new immunofluorescence fixation method. *Mol. Biochem Parasitol.* **137**, 13–21 (2004).
49. Zeeshan, M. et al. Plasmodium ARK2 and EB1 drive unconventional spindle dynamics, during chromosome segregation in sexual transmission stages. *Nat. Commun.* **14**, 5652 (2023).
50. Kumar, S. et al. PfCDPK1 mediated signaling in erythrocytic stages of Plasmodium falciparum. *Nat. Commun.* **8**, 63 (2017).
51. Ekka, R., Gupta, A., Bhatnagar, S., Malhotra, P. & Sharma, P. Phosphorylation of Rhoptry Protein RhopH3 Is Critical for Host Cell Invasion by the Malaria Parasite. *mBio*, https://doi.org/10.1128/mBio.00166-20 (2020).
52. Hobson, B. D., Kong, L., Hartwick, E. W., Gonzalez, R. L. & Sims, P. A. Elongation inhibitors do not prevent the release of puromycylated nascent polypeptide chains from ribosomes. *Elife*, https://doi.org/10.7554/eLife.60048 (2020).
53. Kim, D., Paggi, J. M., Park, C., Bennett, C. & Salzberg, S. L. Graph-based genome alignment and genotyping with HISAT2 and HISAT-genotype. *Nat. Biotechnol.* **37**, 907–915 (2019).
54. Love, M. I., Huber, W. & Anders, S. Moderated estimation of fold change and dispersion for RNA-seq data with DESeq2. *Genome Biol.* **15**, 550 (2014).
55. Bansal, P. et al. Protein kinase TgCDPK7 regulates vesicular trafficking and phospholipid synthesis in Toxoplasma gondii. *PLoS Pathog.* **17**, e1009325 (2021).
56. Wright, M. H. et al. Validation of N-myristoyltransferase as an antimalarial drug target using an integrated chemical biology approach. *Nat. Chem.* **6**, 112–121 (2014).

Acknowledgements

Studies were supported by grant CRG/2021/000147 from Science and Engineering Research Board (SERB), Department of Science and Technology, India and a Team Science grant (IA/TSG/21/1/600261) to PS and TSKP from DBT-Wellcome Trust India Alliance and funds from NII core. PS is a recipient of J.C. Bose Fellowship. The efforts made by Devanshi Sharma, Saakshi Chaudhary in RNAseq data analysis and Mamatharani DV for assistance in RNAseq library preparation and and Manish Kumar in critically reading the manuscript are appreciated.

Author contributions

A.R., N.A., M, B.D, A.B.R performed most experiments and analyzed the data. A.N. assisted in U-ExM and image analysis. B.D. performed transcriptomics under supervision of K.K. N.K. supervised and performed the transcriptomic analysis. N.A. and A.B.R were involved proteomics studies which were supervised and analyzed by T.S.K.P. P.S. designed, supervised and analyzed all parasite-related studies.

Competing interests

The authors declare no competing interests.

Additional information

Supplementary information The online version contains supplementary material available at https://doi.org/10.1038/s41467-025-59476-w.

Correspondence and requests for materials should be addressed to Pushkar Sharma.

Peer review information *Nature Communications* thanks Rita Tewari who co-reviewed with David Guttery, and the other, anonymous, reviewer(s) for their contribution to the peer review of this work. A peer review file is available.